Instituto de Física Teórica
Universidade Estadual Paulista

DISSERTAÇÃO DE MESTRADO IFT-D.016/20

Aging as a Strategy to Prevent Extinction in Microbial Ecosystems

Jairo Martin Rojas Huamaní

Orientador
Ricardo Martínez-García

Agosto de 2020

Rojas Huamaní, Jairo Martin.
R741a Aging as a strategy to prevent extinction in microbial ecosystems / Jairo Martin Rojas Huamaní. – São Paulo, 2020
68 f. : il.

Dissertação (mestrado) – Universidade Estadual Paulista (Unesp), Instituto de Física Teórica (IFT), São Paulo
Orientador: Ricardo Martínez-García

1. Biofísica. 2. Dinâmica populacional. 3. Envelhecimento. 4. Processo estocástico. I. Título

Sistema de geração automática de fichas catalográficas da Unesp. Biblioteca do Instituto de Física Teórica (IFT), São Paulo. Dados fornecidos pelo autor(a).

Acknowledgments

I would like to thank Ricardo Martínez-García for his patience and willingness to help me in this research. Also, I would like to thank our research group for very helpful discussions, from research to advice on how to present the results.

In this time of pandemic, much of the work presented here was done while I was in quarantine. During this time, I have lived in the house of my friends João Pedro, and Andre Pereira - Tais Bastani, this work is possible thanks to you guys. I would also like to thank all my IFT friends that I have met during this master process, friends who have made of this an unforgettable experience. Finally, I am very grateful to Nathan Berkovits for advising me and allowing me to be part of "Journeys into Theoretical Physics: IFT-Perimeter-SAIFR".

This work was possible thanks to the "Coordenação de Aperfeiçoamento de Pessoal de Nível Superior" CAPES, and the Abdus Salam International Centre for Theoretical Physics, ICTP-SAIFR/IFT-UNESP, FAPESP grant 2016/01343-7. This research was supported by resources supplied by the Center for Scientific Computing (NCC/GridUNESP) of the São Paulo State University (UNESP).

Abstract

Could aging provide survival advantages to a microbial population? In this thesis we explore the notion of aging in microbes, which is very different from aging in multicellular organisms. First, we review the use of stochastic processes and their analytical approaches in the analysis of population dynamics. Finally, with the use of these techniques, we develop a model and use it to investigate whether an aging population may have a survival advantage as compared to non-aging ones, these results could provide us with clues about the origin of aging in macroscopic life.

Key-words: Aging; Senescence; Bacteria; Immortality; Stochastic Simulation; Population Dynamics

Field of knowledge: Biological Physics; Population Dynamics; Evolutionary Dynamics

Resumo

Pode o envelhecimento fornecer vantagens de sobrevivência para uma população microbiana? Nesta tese, exploramos a noção de envelhecimento em micróbios, que é muito diferente de envelhecimento em organismos multicelulares. Primeiro revisamos o uso de processos estocásticos e suas abordagens analíticas na análise da dinâmica populacional. Finalmente, com o uso dessas técnicas, desenvolvemos um modelo e o utilizamos para investigar se uma população idosa pode ter uma vantagem de sobrevivência em comparação com outras que não envelhecem, esses resultados podem nos fornecer pistas sobre a origem do envelhecimento na vida macroscópica.

Palavras-chave: Envelhecimento; Senescência; Bactéria; Imortalidade; Simulação estocástica; Dinâmica populacional

Campo do conhecimento: Física Biológica; Dinâmica de População; Dinâmica Evolutiva

Contents

List of Figures

1 Introduction

Sooner or later, without exception, the destiny of every human being is death. Even under ideal conditions, where an infinite amount of resources and protection against environmental hazards are provided, a human will eventually die. This is a consequence of aging, an inevitable characteristic of the human being.

We share this destiny with many other life forms on Earth, and therefore it is natural to believe that aging is a characteristic of all living beings. However, if, as is often argued, nothing in biology makes sense except in the light of evolution [1], and evolution is focused on increasing fitness, then how can aging agree with evolution? Does not aging diminish fitness? The answer should be related to reproductive and survival advantages of aging populations. To answer this question, it is very interesting to recognize the existence of living beings, from the very small, such as bacteria, to those of considerable sizes, such as Hydras, which do not go through senescence, the deleterious effect of aging. In fact, in many theories about the origin of life, an immortal original cellular organism is proposed [2].

Single-celled organisms, such as bacteria, have been a hot topic in recent decades and will be the focus of this thesis. For them, aging is directly related not only to the accumulation of damage over time but also to its reproduction mechanism. Some mother bacteria share half their age in reproduction, turning the original specimen into two identical daughters, while other bacteria have a reproduction strategy closer to the one of the human being, where the mother maintains her age, and the daughter is born with no senescence.

Given the existence of non-aging specimens, the evolutionary forces that led living beings to age are not always present, or some non-aging benefits outweigh them under certain conditions. However, determining these conditions in experimental studies is a challenging task, mainly due to the long time scales in which evolutionary processes such as the emergence of

aging occur. To use theoretical and computational models provides a solution to this problem. Discrete population models are particularly useful when demographic processes, such as reproduction or death, are considered stochastic events at the individual level. Under appropriate mathematical manipulations, it is possible to extrapolate the consequences of these processes to the population level. Using these stochastic frameworks, we can establish individual age-related advantages and observe their effect on the population.

To observe the effects of aging and different reproduction strategies, we developed a stochastic model that mimics the dynamics of a microbial population. We consider the effects of senescence on the mortality rate and how it interacts with different reproductive strategies to determine the size of the population in the stationary-state. Our model also, being stochastic, originates from processes at the individual level, so we have direct control of the parameters used. Using this model, we investigate the benefits that aging offers to populations and analyze the conditions in which aging should or should not appear in microbes.

This thesis is structured in the following way. In section 2 we introduce basic concepts related to aging and its evolutionary origins, senescence, and microbial aging. Then, in section 3 we present a review of the use of stochastic dynamics to study population dynamics. Analytical methods such as the generating function or mean field theory are presented together with the numerical method of Gillespie to simulate the complete stochastic dynamics. In section 4 we present our model and how to obtain predictions from it using analytical and numerical methods. Finally, in section 5 we analyze the effect of aging and how different reproduction strategies affect the persistence of microbial populations. We end this thesis with a discussion of our results and future directions.

2 Aging: Definition and Motivations

2.1 Aging

Aging is a concept deeply present in our minds. One is born without age, and as time passes, one grows older and older. The concept of age, when we think of humans and most multi-cellular life forms, is so tightly related to time that we use it as a synonym. A baby, who is two-year old, is considered young, in contrast to a ninety-year grandfather who is considered old. However, in general, the relationship between age and time is not that simple. Microbes are an excellent example of the existence of more complex relations between age and time. That is why we need a more precise definition of age and how it generally affects living beings.

2.1.1 Causes of Death

To have a precise definition of age, we must first consider death and its causes. Every organism, from the tiniest microbes to the largest animals and plants, are always at risk of dying, and age is related to that. These causes of death can be classified into two categories:

External Hazards

Hazards caused by factors independent to the individual that can eventually kill it. In Fig(1) we summarize these hazards at the level of microscopic dynamics[1], where we identify three classes:

- Related to environmental phenomena. For example, a fire that kills animals in the forest, or a burst in the concentrations of antibiotics used to kill bacteria responsible of infections. In Fig(1), we show an individual who, after the appearance of a "lightning bolt" which is an environmental hazard, disappears, subtracting one individual from the population.

[1]By microscopic dynamics, in this work, we mean a process that is described at the level of individuals, i.e. one specimen being killed, or one giving birth. It is opposed to macroscopic dynamics, where only processes at the population level are described.

- Predation, or more generally, transfer of biomass from lower to higher levels of the trophic chain. As examples, we have the grass as a "prey" of the zebra and the zebra itself as the prey of the lion. In Fig(1) it is represented by the interaction between two individuals from different populations, one brown and one green, which makes one of them disappear.

- Competition for a shared resource between individuals belonging to the same or different species. In this scenario, the limited amount of resources regulates the size of the population. For example, with a limited amount of food, some members of a wolf pack may die due to starvation. In Fig(1), we observe two specimens from the same population, whose interaction results in the survival of only a single individual.

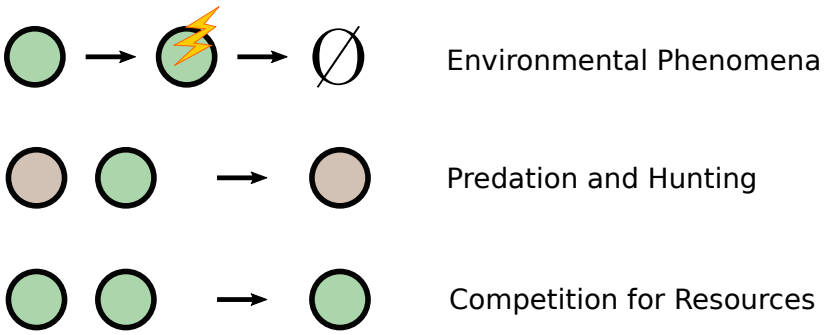

Figure 1: Microscopic representations of the effect of external hazards.

However, even under perfect conditions, where no external hazard is present, organisms die. This is a consequence of the appearance of internal malfunctions.

Internal Malfunctions

Failure of homeostasis, the preservation of the internal condition necessary to keep a living being alive. These errors are caused by the accumulation of damage, which has its origins in mutations and "scars":

- Mutations that affect the function of the organism [3]. A common example of this situation is the appearance of cancer in humans and other multi-cellular organisms.

- "Scars" or failed repairs in the development and recovery of the organism [4][5]. A scar on the skin can be seen as an imperfection, and a similar situation is present within our cells.

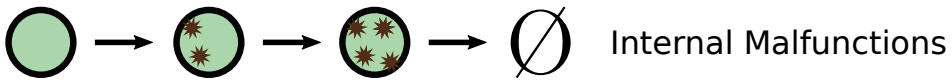

Figure 2: Microscopic representation of the effect of internal malfunctions.

Over time, this damage, quantified by the value of $\mathcal{D}$, accumulates and produces a less efficient internal function, eventually leading to the death of the organism. In Fig(2) we present a schematic representation of this process.

2.1.2 A Definition for Aging

In this work, we define aging as the decrease in the reproductive and survival capacity of an individual, and therefore, it also decreases the fitness of a specimen. Following this definition, consider the following example: Suppose there is a newborn cell at time $t = 0$, with zero damage $\mathcal{D} = 0$. As time passes, our specimen accumulates damage, represented by brown stars in Fig(3), as a result of homeostatic processes.

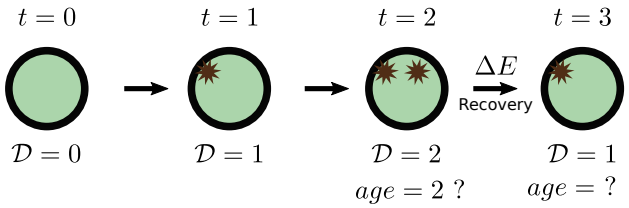

Figure 3: In order to define age, we have to relate it to time or to accumulated damage.

At time $t = 1$, the cell has accumulated damage $\mathcal{D} = 1$ and, at time $t = 2$ damage $\mathcal{D} = 2$. Since the accumulated damage increases by one at $\Delta t = 1$, we might be tempted to define the age of our specimen equal to the elapsed time t since its birth. This is, for instance, the case in humans, since the accumulated damage always increases with time [6]. However, the monotonic growth of $\mathcal{D}$ is not universal and it is, indeed, not present in many microorganisms.

In these living beings, for example, throughout their life cycles, they may decide to allocate part of their energy to rebuild or repair damaged structures. This is illustrated in Fig(3) by the reduction in the number of brown stars between $t = 2$ and $t = 3$. Finally, this damage reallocation can also be result of different reproduction strategies.

Following the definition of aging as decrease in survival capabilities, and considering the organism in Fig(3) which is less likely to die due to internal malfunctions at time $t = 3$ than at time $t = 2$, we say that the organism is younger at $t = 3$, than at $t = 2$. **Following this reasoning, we conclude that the age of our living being is not quantified by the time elapsed since birth, but by the accumulated damage** $age = \mathcal{D}$. It should be noted that the age of an organism in our model could decrease over time.

Finally, following this definition of aging, we call immortal specimens to those specimens that have a bounded age, for example a specimen that is born with $\mathcal{D} = 2$ and reproduces dividing its damage symmetrically every time it reaches $\mathcal{D} = 4$ so it has $\mathcal{D} = 2$ after each reproduction process, and $\mathcal{D} \in [2, 4]$. This definition is opposed to that of mortal living beings which are specimens that have an unbounded age, like the case of human beings were age increases monotonically until death. In this sense, even if a specimen is what we call immortal, it can die due to external hazards, competition, or even internal malfunctions present in its available age ranges, but it can not be arbitrarily old.

2.2 Origins of Aging

The seemingly contradiction between the effects of aging on fitness and its recurrent evolutionary success across the tree of life has led to several theoretical attempts to explain the origin and evolutionary stability of aging [7][8]. In this section, before moving on to more technical aspects of our study, we review some of the strongest hypotheses[2][9][10].

2.2.1 Resources Limitations

At the individual level, a specimen has a limited amount of energy that has to be allocated to perform several tasks, such as protection, feeding, reproduction, and self-maintenance. If the latter did not require effort, a contradiction between aging and evolution would arise, because populations without internal malfunctions are less likely to die, and therefore they produce off-springs over a longer time than mortal ones, resulting in populations with higher fitness. This is the origin of the apparent contradiction presented above. However, there is an amount of energy needed to recover, and the more you invest in it, the less you will invest in other functions.

Only taking into account the processes of reproduction and self-maintenance, we find that different species, led by evolution, search for the optimal allocation of limited internal resources in each of these tasks [11][12]. If members of a species invest heavily in repair and live a long time, then they reproduce later and their chances of dying due to events beyond their control increase. Take, for example, an animal $\mathcal{A}$ that spends most of its energy in repairing internal damage, and, as a result, it has fewer resources available to grow and takes longer to reach sexual maturity compared to other species $\mathcal{B}$ with a shorter lifespan. In this scenario, $\mathcal{B}$ does not only have an advantage in terms of population growth rate, but it also has a higher probability of producing offspring before an external hazard kills it. Remember that the presence of external hazards do not depend on the way individuals age, and therefore affect in the same way individual $\mathcal{A}$ and $\mathcal{B}$. If the probability of dying as a result of an external hazard is considered constant over time, the chances that a given individual is alive at a time t decrease exponentially with t. Therefore, the evolutionary trade-off between reproducing earlier and dying sooner and reproducing later and dying later explains the emergence of aging.

2.2.2 Mutation Pressure

Assuming that the probability of dying as a result of a external hazard is constant over time, the number of individuals from older generations is exponentially smaller compared to the number from new ones. Therefore, the majority of newborn cells will be the result of the reproduction of new generations and natural selection will focus mainly on the genes of young parents. As a consequence, for example, mutations that appear and cause little benefits to young organisms but have deleterious effects in older populations [13][14], would still have possibilities to spread to new generations and be natural selected. On the other hand, genes that benefit older populations and that could lead to immortality, even if they do not affect young members of the population, will have a hard time propagating and being selected for evolution, due to the relative small number of old members in this population.

2.2.3 Faster Adaptability

Finally, an important advantage experienced by organisms that allocate resources to reproduction instead of maintenance [14], is that short generation times can accelerate evolution and therefore provide faster adaptability to changing environmental conditions. This is especially important in highly erratic environments where adaptation is required in short periods. An example of these advantages is present in bacteria which have shown rapid adaptation to changes in antibiotic concentrations. Regardless of whether bacteria have a long lifetime under ideal conditions or not, they are prone to dying from antibiotics with the same chances. If bacteria take considerable time to reproduce, a periodical treatment could lead them to extinction since they do not have chances of accumulating mutations and adapt to the presence of antibiotics in the extracellular medium, something that fast-reproducing bacteria are able to do.

It should be noted that these hypotheses are not mutually exclusive and we expect that the consequences of all these processes add up. However, despite the presence of these advantages, some living beings, from microbes to larger organisms like the hydra, have developed

"immortality", or not aging features. In this context, an interesting question may arise: are there limits when aging is better than immortality and vice versa? What are these limits? Should they be given by the environment, internal competition, or a combination of them? In this thesis we develop a new mathematical approach to answer these questions. Specifically, in section 4 we present the framework and in section 5 we answer these questions by focusing on whether or not aging provides survival benefits to populations under environmental conditions.

2.3 Aging in Microorganisms

A few decades ago, microorganisms were commonly believed to be "immortal" or, in other words, that their accumulation of damage, $\mathcal{D}$, were bounded, and therefore, they did not "age" to be very old. This belief was based in two reasons:

- In symmetric reproduction, cell material is duplicated before division, and because this division is symmetric, both resulting cells get the same amount of new and old material. This process eventually makes the original cell younger after each reproduction process, and bounds the range of ages of the species.

- As mentioned earlier, for microbes, the number of individuals in older generations is exponentially smaller than in younger generations. Taking this into account, and that the reproduction characteristic timescale is quite short in cells, we have a tremendous ratio between the members of young and old generations. As a consequence, in bacteria colonies, it has been very difficult to observe specimens with large age, since the younger ones overwhelmed them in number.

2.3.1 Strategies of Reproduction

Symmetric Reproduction

If mitosis is completely symmetric, the damage accumulated by a parent cell is shared equally

between the two daughters, this leads to a cell division process as shown in Fig(5). This scenario results in a bounded age range and as a consequence, an immortal population emerges as observed in Fig(5), where, for simplicity, we fixed the time required for reproduction, or generation time, to $2\Delta t$, a time that determines the values between which the specimen age oscillates. Here we observe that, even after several generations, all the individuals present in the population have had a maximum of $\mathcal{D} = 4$, just before reproducing, and a minimal age of $\mathcal{D} = 2$, which makes the specimen immortal as shown in the Fig(6).

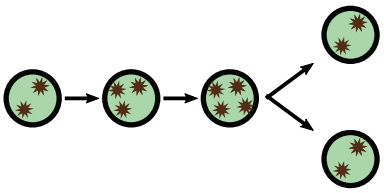

Figure 4: Microscopic representation of symmetric reproduction.

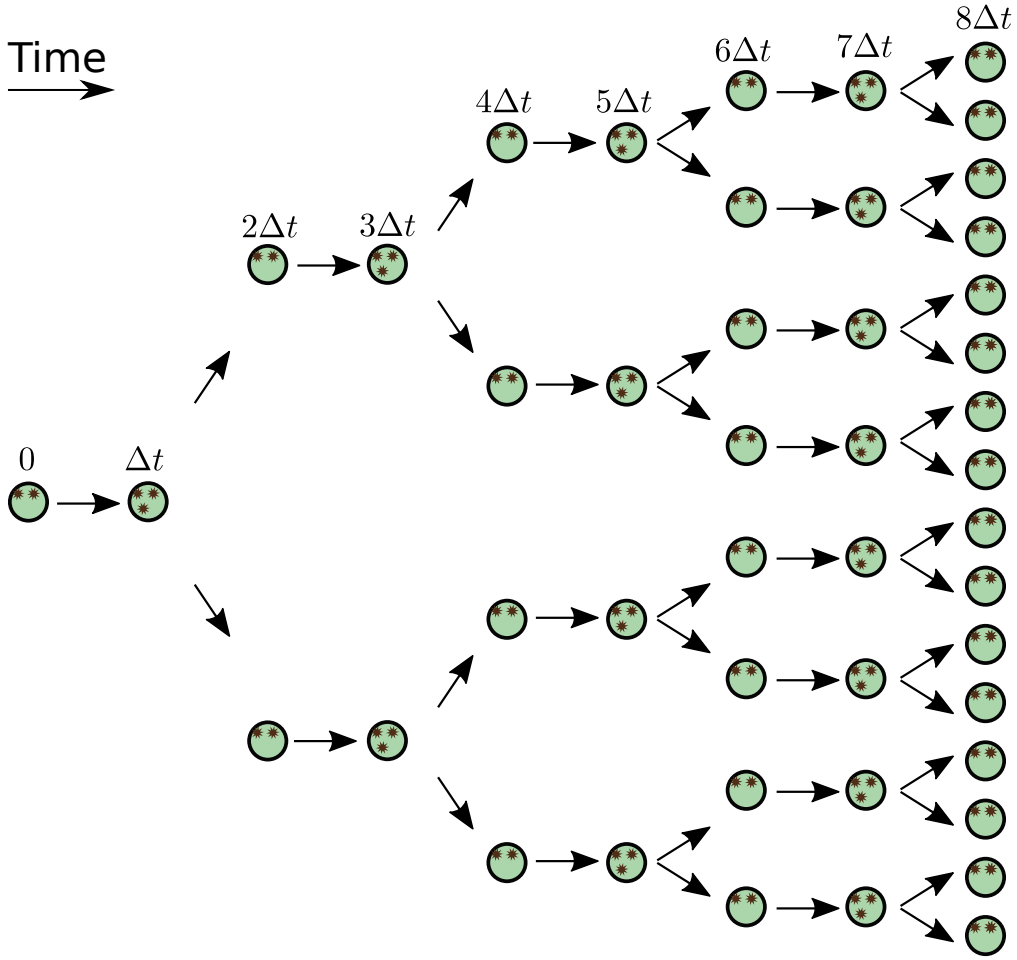

Figure 5: Population dynamics for a population with symmetric reproduction and fixed Δt.

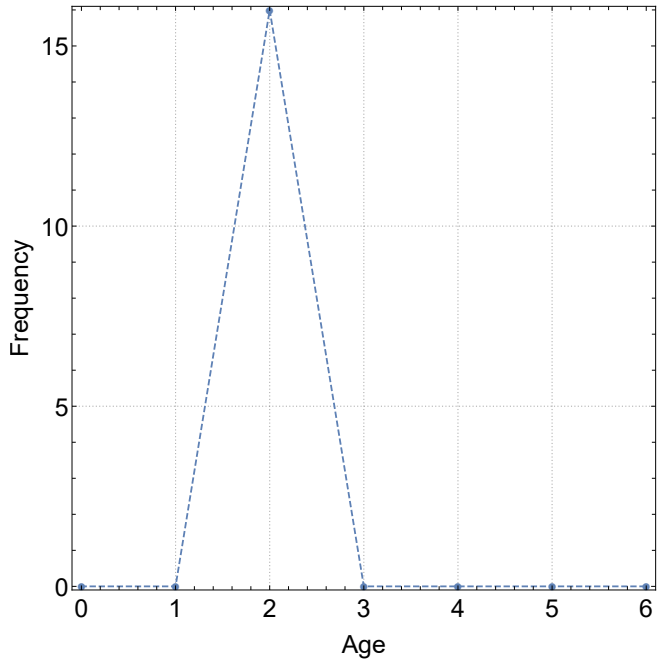

Figure 6: Age distribution of the population of Fig(5) at time $t = 8\Delta t$.

Asymmetric Reproduction

In contrast to the symmetric reproduction strategy, the asymmetric reproductive parent cell retains the total damage accumulated while giving birth to a daughter, which is born with no damage [15] as shown in Fig(7). Here we see a clear difference between the two cells that result from the reproductive event, and it is very intuitive to think about one cell as the "mother" and the other as the "daughter". The former is the one that keeps all the damage, while the latter is the one that receives all the new DNA and structures. This way of distributing damage, and therefore age, is very similar to that followed by humans and most multi-cellular organisms.

Asymmetric reproduction allows a diversity of ages [16] in the population, even when generation times are fixed, which is the case for Fig(8). Here we observe that the age of the members vary from $\mathcal{D} = 0$ to $\mathcal{D} = 6$. If only internal malfunctions are considered as the causes of death, we expect the age distribution to behave as an exponential, and Fig(9) shows that individuals tend to accumulate at lower ages, although the exponential behavior is not observed due to the low number of cells considered in the population of Fig(8).

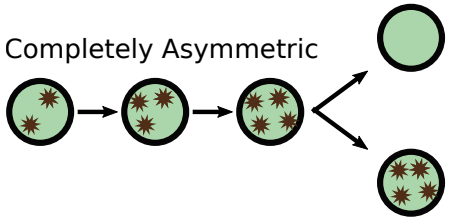

Figure 7: Macroscopic representation of symmetric reproduction.

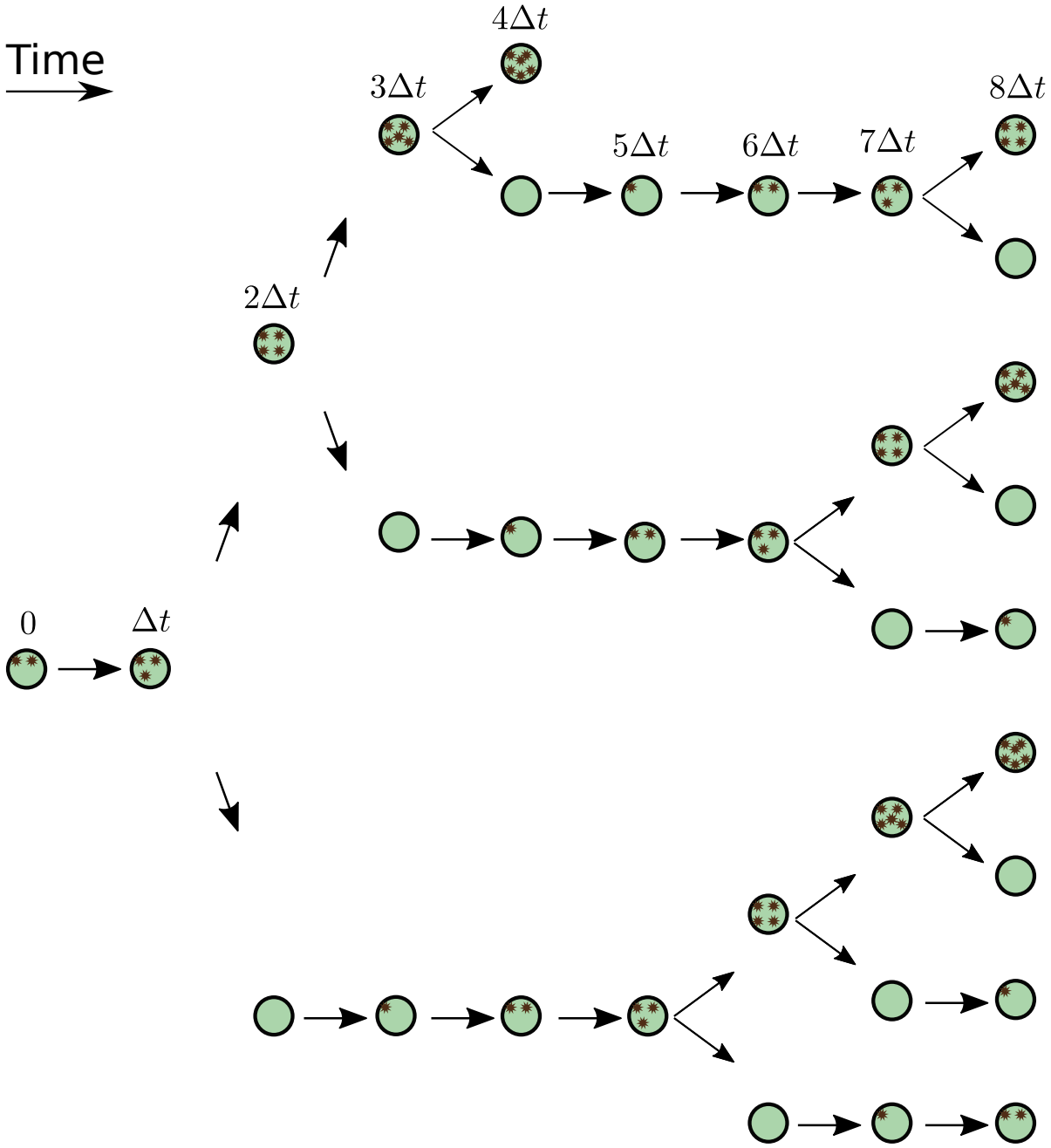

Figure 8: Population dynamics given asymmetric reproduction.

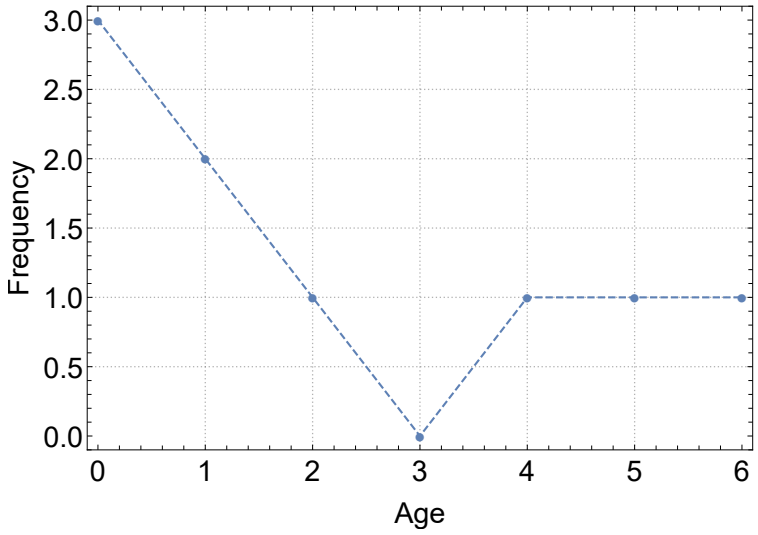

Figure 9: Age distribution of a population with asymmetric reproduction.

Partially Asymmetric Reproduction

It is important to know that the symmetric and asymmetric reproduction are not isolated strategies. There is a continuum of reproductive strategies defined by the fraction of the damage that goes to each cell. Strategies within this continuum can be labeled by a single parameter μ between 0.5 and 1, where 0.5 means symmetric reproduction, and 1 means asymmetric reproduction, which are probably evolutionary connected through a smooth transition. As a consequence, we also have populations with partially asymmetric reproduction strategies as shown in Fig(10), where the damage is shared, but not in equal amounts between the daughters.

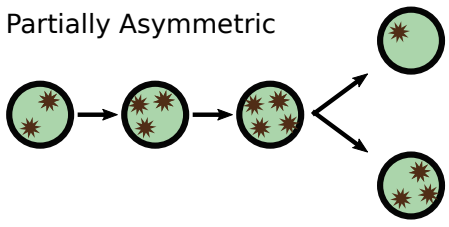

Figure 10: Microscopic representation of partially asymmetric reproduction.

2.3.2 Biological Mechanisms of Sharing Aging

Symmetric and asymmetric reproduction, as well as all the other strategies that lie in the continuous spectrum between them, are better understood in microbes [17]. There are different mechanisms to achieve these strategies, where microorganisms sequester the damage in their daughters, for example:

- Morphological asymmetric reproduction[18]

  A paradigmatic example of a microorganism that uses this strategy is *Saccharomyces cerevisiae*, a yeast widely used by humans in the production of wine and bakery. Here, the parent cell places all its damage on the daughter.

  In Fig(11) we can observe that the original cell has high damage inside, represented by darkness, and divides its nucleus in two while the damage is actively secreted in one region. Later, organelles are also formed in this region, and a "wall" is built at the neck of the partition. Once this process is complete, we find that one of the daughter cells is similar in size to the original one, but it is younger, along with a smaller daughter cell with most of the damage.

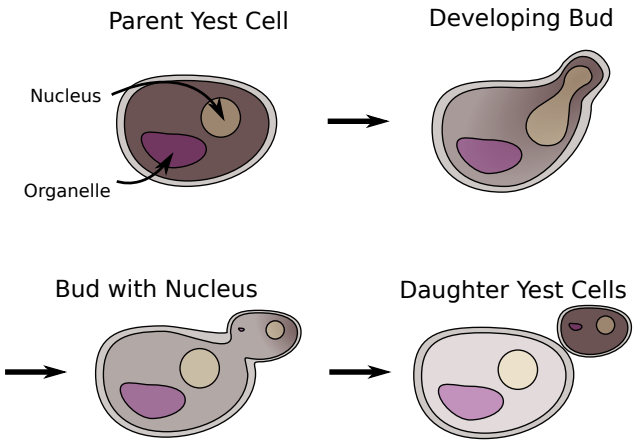

Figure 11: Morphological asymmetric reproduction.

- Cryptic asymmetric distribution

  This is a method used by *Escherichia Coli*, a bacterium generally found in the digestive

system of mammals. Take, as an example, one of these bacteria with age zero, with the restriction that they reproduce every Δt and that in this time interval they accumulate a certain level of internal damage, represented by two brown stars. As we can see in Fig(12), after a time Δt the *E. Coli* cell has spread its damage on two opposite poles and then splits in the middle so that the damage is distributed equally between the two daughters. However, an asymmetry begins to appear in the next generations because the mothers, after another Δt, have different damage in each pole, resulting in daughters with different ages.

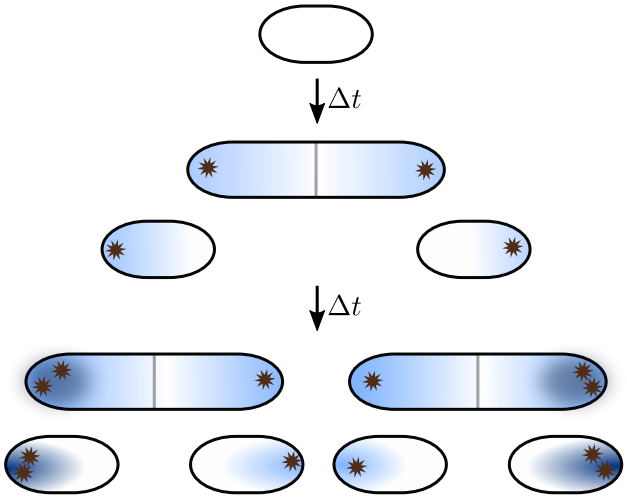

Figure 12: Cryptic asymmetric distribution

2.3.3 Different Aging Distributions and Dominance of one Reproduction Strategy

Looking back at the different reproduction strategies, we find two clear ways in which cells can distribute their internal damage upon division, which are symmetric and asymmetric reproduction, along with a continuous connection between them. We observe that asymmetric reproduction leads to our standard concept of aging, similar to humans aging, and symmetric reproduction, by not allowing great age variation, confers "immortality" on the individual. It is worth noting that we expect a continuous transition between these reproductive strategies, as represented by the full spectrum of partially asymmetric distribution.

Each of these strategies leads to a different age distribution within the population. For example, we show in Fig(13) a superposition of the normalized population age distributions presented in Fig(6) and Fig(9). Finally, as a key part of this work, the shape of the distributions could be beneficial/detrimental to the total population, so a question may arise: does each of the reproductive strategies, as represented by different age distributions, provide survival benefits to populations in different environmental contexts?

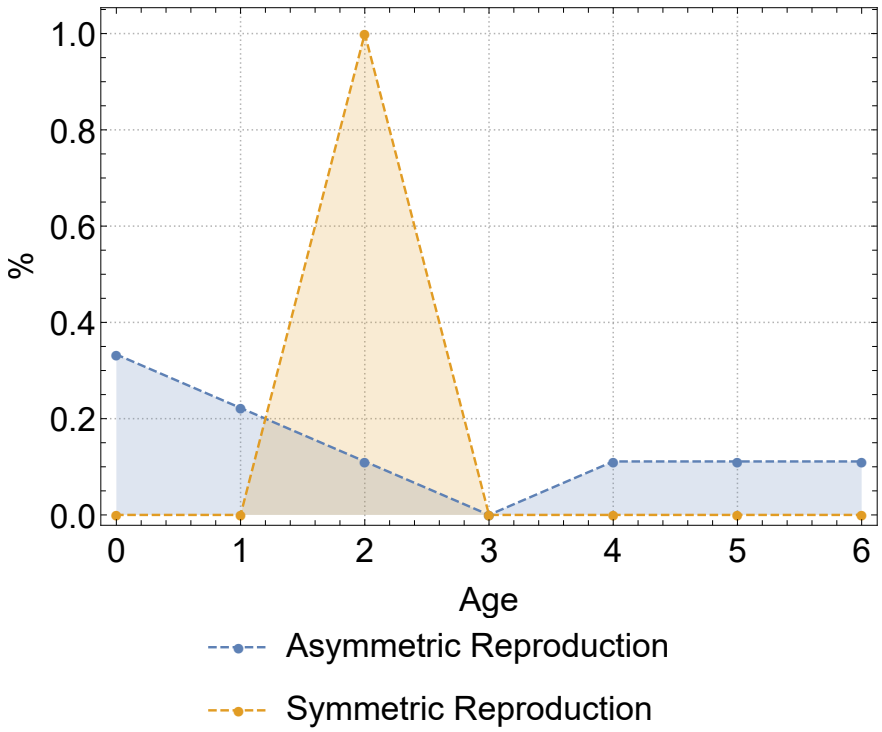

Figure 13: Age distribution for symmetric and asymmetric reproduction.

3 Population Dynamics with Stochastic Processes

In this section we provide a brief review of the most important concepts and tools in the study of population dynamics. We first revisit the two simplest growth models for single-species populations: exponential and logistic growth. We then show how these model can be derived from the *microscopic* interactions that occur at the level of the individuals that constitute the population.

3.1 Short Overview on Population Dynamics.

3.1.1 Exponential Growth

We explore the exponential growth, which is the simplest population dynamics [19]. For many microorganisms, such as bacteria or yeast, reproduction consists of a parent cell that divides into two. We referred to the average time it takes for a new daughter cell to grow and divide as the generation time t_r .

If we fix t_r to a constant for each member of the population, and n_0 the initial number of members, our reproduction process will follow a geometric progression:

$$n(t) = n_0 2^{t \backslash t_r}, \tag{3.1}$$

where $\backslash$ represents integer division. On the other hand, if we consider the population number $n(t)$ as a continuous, where the integer division is no longer a problem, the growth will be exponential [20]:

$$\begin{aligned} n(t) &= 2^{\frac{t}{t_r}} n_0 \\ &= e^{\frac{ln(2)}{t_r} t} n_0 \\ &= e^{rt} n_0, \end{aligned} \tag{3.2}$$

where we have defined $r = ln(2)/t_r$ as the birth rate per bacteria. Both growth dynamics are compared in Fig(14).

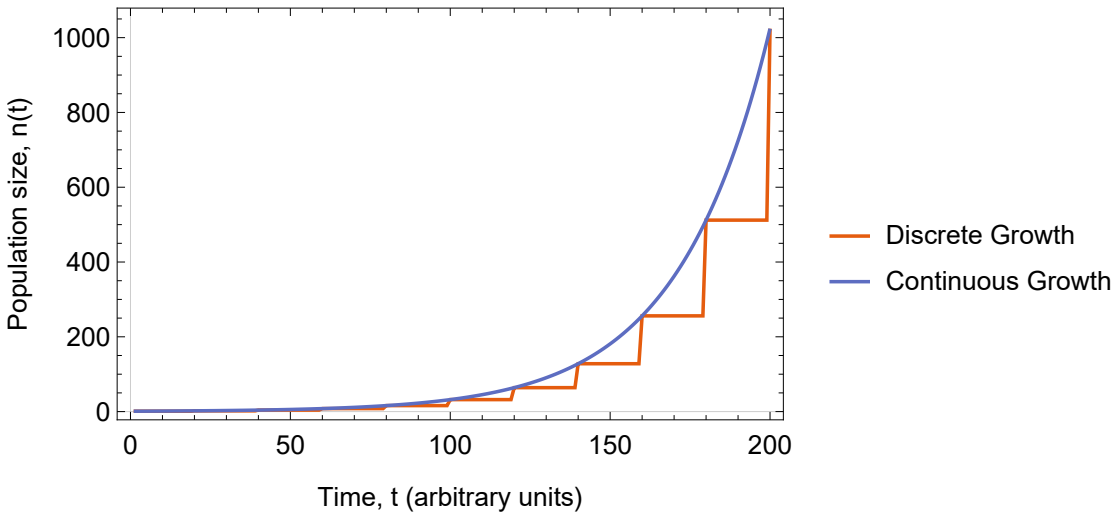

Figure 14: Continuous and discrete (geometric progression) population growth for a $r_{\text{eff}} = ln(2)/20$.

We can add a death rate per bacteria d. It will affect growth curves in a similar way to r, but with opposite sign. Therefore, we can define the difference between r and d as the effective growth rate per bacteria r_{eff} and the population will continue to grow exponentially but with a different characteristic time scale:

$$n(t) = e^{(r-d)t} n_0. \tag{3.3}$$

Finally, the reproduction-death process can be written in terms of an ODE of which the Eq. 3.3 is the solution to this reproduction-death process. In this ODE, population growth rate is proportional to the total number of individuals $n(t)$:

$$\begin{aligned} \frac{d}{dt} n(t) &= (r-d) n(t) \\ &= r_{\text{eff}}\ n(t). \end{aligned} \tag{3.4}$$

3.1.2 Logistic Growth

Exponential growth is a good model for populations when there is no shortage of resources for individuals. However, one of its consequences is that $n(t)$ can grow infinitely, this being an unrealistic scenario because the resources necessary for growth will eventually become scarce. To consider resource limitation, we can add a negative quadratic term to the differential equation 3.4 [19]:

$$\frac{d}{dt}n(t) = r\ n(t) - \frac{r}{K}n(t)^2. \tag{3.5}$$

Here, the constant K is called the carrying capacity and is the non-trivial stable fixed point of the equation. The differential equation for logistic growth can be solved analytically:

$$n(t) = \frac{K n_0\ e^{rt}}{K + n_0(e^{rt} - 1)}. \tag{3.6}$$

As this analytical solution shows, for small values of $n(t)$, which are present at small times for small values of n_0, our growth is exponential. Finally, as $n(t)$ increases, it converges to K as can be see in Fig(15).

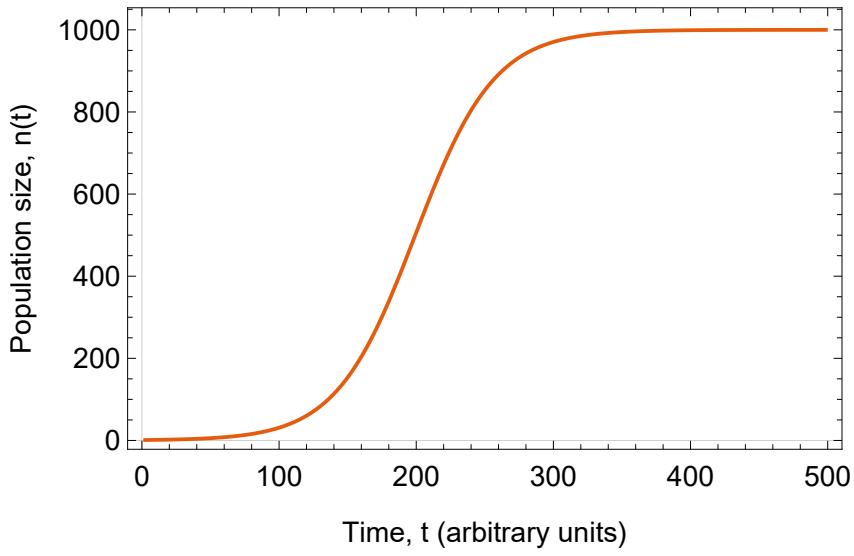

Figure 15: Logistic growth for a $r_{\text{eff}} = ln(2)/20$ and $K = 10^3$.

3.2 Population Dynamics From A Stochastic Point of View

3.2.1 Microscopic Dynamics

Macroscopic dynamics are changes on populations as a whole, and microscopic dynamics are processes at the level of individuals. The most important microscopic processes that we will consider here are three, summarized in Fig(16).

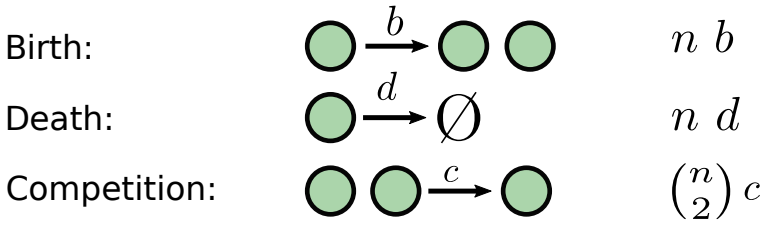

Figure 16: Three main microscopic processes that affect the dynamics of a single-species microbial population.

Birth

Although sexual reproduction has also been observed in microorganisms [21], in this work we will only consider microbial populations with asexual reproduction. Asexual reproduction will occur driven by genome replication followed by cell division, so each time this process takes place, two daughter cells will result from one mother cell, and the total population will increase by one. Since birth only depends on the number of potential mothers, the probability of having a new birth is given by its number n multiplied by the birth rate per individual b.

Death

This is analogous to the birth process but with the opposite effect on population size. Cell death events represent processes in which an individual disappears as a result of environmental hazards, predation, or internal malfunction. As we do not consider changes in the intensity of external factors that may cause cell death, the mortality rate per individual is a constant d. The chances of the population to have a death are d multiplied by the total number n of individuals.

Competition

This is a process similar to death and has the same consequence, the removal of an individual from the population. Competition is the result of the interaction of a pair of individuals from the populations under study, where one of them results in death. For single-species populations the probability of observing a competitive interaction is proportional to the competition rate c and the number of possible combinations in the population: $\binom{n}{2}$. On the other hand, if we consider more than one species, for example two species labeled by A and B respectively, the probability of observing a competitive interaction also considers then interaction between their members: $c\ n_A n_B$.

3.2.2 The Master Equation

Starting from the microscopic dynamics in terms of the events described in 3.2.1, we can construct a probabilistic description of the population dynamics using the master equation. A master equation is a dynamic equation that describes how the probability $P(n,t)$ of having a population of size n at time t, evolves with time. Next, we will see how this probabilistic description can be derived from the microscopic rates introduced above. To this end, we will assume that we know all the microscopic rates (birth, death, and competition) as well as the size of the population at time t. Then it is possible to calculate the probability of finding a given population size n at time $t + dt$ by considering all the possible events that can occur within the time interval dt and influence the population size.

First, we must consider the probability that no microscopic event is recorded between t and $t + dt$. The probability of maintaining the initial number n is given by one minus the probability of some microscopic event occurring:

$$P(n, t + dt \mid n, t) = 1 - n\ b\ dt - n\ d\ dt - \binom{n}{2}\ c\ dt. \tag{3.7}$$

Second, we consider the probability that one individual will be added to the population due

to reproduction:

$$P(n, t + dt \mid n - 1, t) = (n - 1)\ b\ dt. \tag{3.8}$$

Finally, we compute the probability that the population will decrease by one:

$$P(n, t + dt \mid n + 1, t) = (n + 1)\ d\ dt + \binom{n+1}{2}\ c\ dt. \tag{3.9}$$

Putting together all the terms that correspond to each of the possible events that can make the population size to be equal to n at time $t + dt$, we obtain:

$$\begin{aligned} P(n, t + dt) =& P(n, t)P(n, t + dt \mid n, t) + P(n + 1, t)P(n, t + dt \mid n + 1, t) \\ &+ P(n - 1, t)\ P(n, t + dt \mid n - 1, t) \\ =& P(n, t) \left(1 - n\ b\ dt - n\ d\ dt - \binom{n}{2}\ c\ dt\right) \\ &+ P(n + 1, t) \left((n + 1)\ d\ dt + \binom{n+1}{2}\ c\ dt\right) \\ &+ P(n - 1, t)\ (n - 1)\ b\ dt. \end{aligned} \tag{3.10}$$

Taking the limit $dt \to 0$ on Eq. 3.10 we obtain:

$$\begin{aligned} \frac{d}{dt}P(n, t) =& - P(n, t) \left(n\ b + n\ d + \binom{n}{2}\ c\right) \\ &+ P(n + 1, t) \left((n + 1)\ d + \binom{n+1}{2}\ c\right) \\ &+ P(n - 1, t)\ (n - 1)\ b, \end{aligned} \tag{3.11}$$

which is the master equation of the system. Note that we have not made any approximation so far and hence if we are able to solve the master equation and thus obtain $P(n, t)$ for all t, we have a complete description of the stochastic population dynamics. However, as we will discuss in the following sections, obtaining this solution is a difficult and often impossible task.

3.3 Analytic Methods

Here we present two different analytical approaches to get information from the master equation using the generating function and the mean-field theory approach [22][23][24].

3.3.1 The Generating Function

A standard method to solve the master equation is to define a generating function $G(s,t)$, a function of time t and an auxiliary variable s:

$$G(s,t) = \sum_{n=-\infty}^{\infty} s^n P(n,t). \tag{3.12}$$

For populations we have $P(n,t) = 0$ for $n < 0$ and therefore $G(s,t)$ is a series of powers of s with positive exponent and coefficients $P(n,t)$:

$$G(s,t) = P(0,t) + s\ P(1,t) + s^2\ P(2,t) + s^3\ P(3,t) + \ldots. \tag{3.13}$$

Therefore, it is possible to calculate $P(n,t)$ by expanding $G(s,t)$ on s around 0 and taking the corresponding coefficient.

The generating function is also useful for calculating different moments of probability distribution without an explicit calculation of the probabilities $P(n,t)$. For example, we can calculate the mean population size $< n(t) >$ using:

$$\begin{aligned} < n(t) > &= \sum_n n\ P(n,t) \\ &= \sum_n \frac{d}{ds} s^n P(n,t)\bigg|_{s\to 1} \\ &= \frac{d}{ds} \sum_n s^n P(n,t)\bigg|_{s\to 1} \\ &= \frac{d}{ds} G(s,t)\bigg|_{s\to 1} \end{aligned} \tag{3.14}$$

Similarly, we can get the second moment $< n(t)^2 >$ as:

$$< n(t)^2 >= \frac{d}{ds}\left(s \ \frac{dG(s,t)}{ds} \right)\Big|_{s=1} \tag{3.15}$$

Let us consider a microscopic dynamics with processes of birth and death (and no competition). The dynamics of the population is described by the following master equation:

$$\frac{dP(n,t)}{dt} = - \ P(n,t)n(b+d) + P(n+1,t)(n+1) \ d + P(n-1,t) \ (n-1) \ . \tag{3.16}$$

After taking the product of the master equation with s^n and adding over n we identify a dynamic equation for the generating function:

$$\begin{aligned}
\frac{dG(s,t)}{dt} &= \sum_n s^n \frac{dP(n,t)}{dt} \\
&= \sum_n s^n \left(-P(n,t)n(b+d) + P(n+1,t)(n+1) \ d + P(n-1,t) \ (n-1) \ b \right) \\
&= \sum_n \left(-s^n P(n,t)n(b+d) + s^{n-1} P(n,t)n \ d + s^{n+1} P(n,t) \ n \ b \right) \\
&= -(b+d)s\frac{d}{ds}G(s,t) + d\frac{d}{ds}G(s,t) + b \ s^2 \frac{d}{ds}G(s,t).
\end{aligned} \tag{3.17}$$

This equation can be solved up to a constant which is obtained using our initial condition $n(t) = n_0$:

$$G(s,0) = s^{n_0}. \tag{3.18}$$

Note that by introducing the generating function, we have transformed a infinite system of coupled ODEs (one for each $P(n,t)$) into a partial differential equation. The PDE at Eq. 3.17 can be solved using standard methods, such as the method of the characteristics where we convert Eq. 3.17 into ODEs along a curve parametrized by x such that $G(s,t)$ is constant

along the curve:

$$\begin{aligned}\frac{d}{dx}G(s(x),t(x)) &= F(G(s(x),t(x)),s(x),t(x)) \\ &= \frac{\partial}{\partial s(x)}G(s(x),t(x))\frac{d}{dx}s(x) + \frac{\partial}{\partial t(x)}G(s(x),t(x))\frac{d}{dx}t(x),\end{aligned} \tag{3.19}$$

with

$$F(G(s(x),t(x)),s(x),t(x)) = 0. \tag{3.20}$$

We identify:

$$\begin{aligned}\frac{d}{dx}s(x) &= (b+d)s(x) - d - bs(x)^2 \\ \frac{d}{dx}t(x) &= 1,\end{aligned} \tag{3.21}$$

which are ODEs with solutions:

$$\begin{aligned}s(x) &= \frac{e^{b(x+c_1)} - de^{d(x+c_1)}}{e^{b(x+c_1)} - be^{d(x+c_1)}} \\ t(x) &= x.\end{aligned} \tag{3.22}$$

Now, we can get $s(t)$ from $s(0)$:

$$s(t) = \frac{d-b}{\frac{(d-bs(0))e^{t(b-d)}}{s(0)-1} + b} + 1, \tag{3.23}$$

or, inverting Eq. 3.23 we can get $s(0)$:

$$s(0) = \frac{d(s-1)e^{t(b-d)} - bs + d}{b(s-1)e^{t(b-d)} - bs + d} \tag{3.24}$$

To compute $G(s(x),t(x))$, we need to go to the origin of the curve and compute $s(0)^{n_0}$:

$$\begin{aligned} G(s,t) &= G(s(x),t(x)) \\ &= G(s(0),t(0)) \\ &= G(s(0),0) \\ &= s(0)^{n_0} \\ &= \left(\frac{d(s-1)e^{t(b-d)}-bs+d}{b(s-1)e^{t(b-d)}-bs+d}\right)^{n_0} \end{aligned} \tag{3.25}$$

Now, with an analytic expression for $G(s,t)$ we are able to compute $P(n,t)$:

$$\begin{aligned} P(0,t) &= \left(\frac{d\left(e^{t(b-d)}-1\right)}{be^{t(b-d)}-d}\right)^{n_0} \\ P(1,t) &= \frac{n_0(b-d)^2e^{t(b-d)}\left(\frac{d\left(e^{t(b-d)}-1\right)}{be^{t(b-d)}-d}\right)^{n_0-1}}{\left(d-be^{t(b-d)}\right)^2} \\ P(2,t) &= \frac{n_0(b-d)^2e^{t(b-3d)}\left(\frac{d\left(e^{bt}-e^{dt}\right)}{be^{bt}-de^{dt}}\right)^{n_0}\left(\left(n_0(b-d)^2-(b+d)^2\right)e^{t(b+d)}+2bd\left(e^{2bt}+e^{2dt}\right)\right)}{2d^2\left(e^{t(b-d)}-1\right)^2\left(d-be^{t(b-d)}\right)^2}\ldots, \end{aligned} \tag{3.26}$$

which are shown in Fig(17) and Fig(18).

Finally, we are also able to compute the 1^{st} and 2^{nd} moment:

$$\begin{aligned} <n(t)> &= n_0e^{(b-d)t} \\ <n^2(t)> &= \frac{n_0e^{t(b-2d)}\left(e^{bt}(bn_0+b-dn_0+d)+(-b-d)e^{dt}\right)}{b-d} \end{aligned} \tag{3.27}$$

We observe that the mean follows an exponential, which is the macroscopic dynamics that we expect for a population with only birth/death processes. Also, we obtain an expression for the standard deviation of this growth. We show these two moments in Fig.(18).

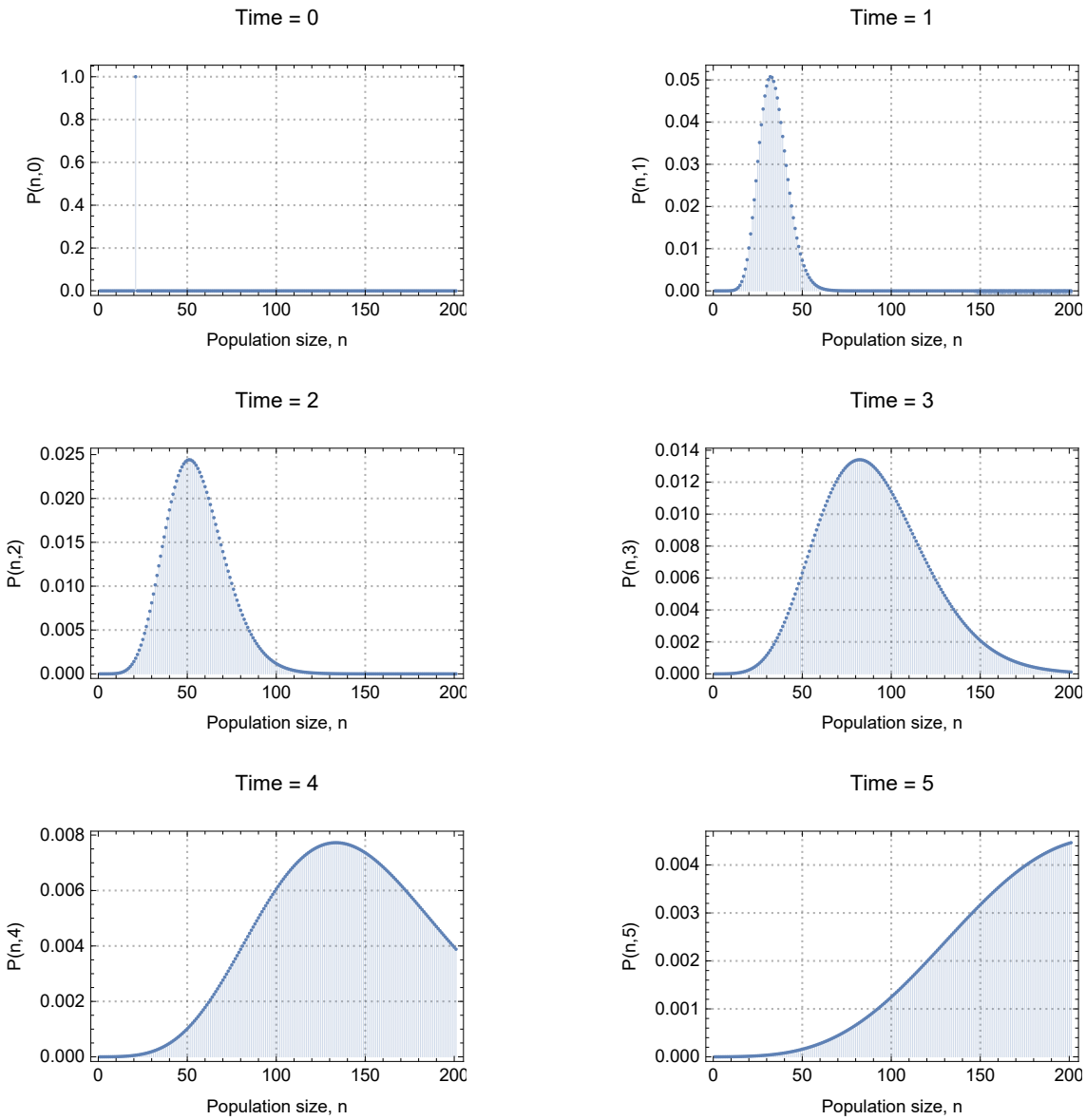

Figure 17: Analytical solution of $P(n,t)$ for $0 < t < 5$. The parameters of the population dynamics are $n_0 = 20$ and $r_{\text{eff}} = \frac{1}{2}$.

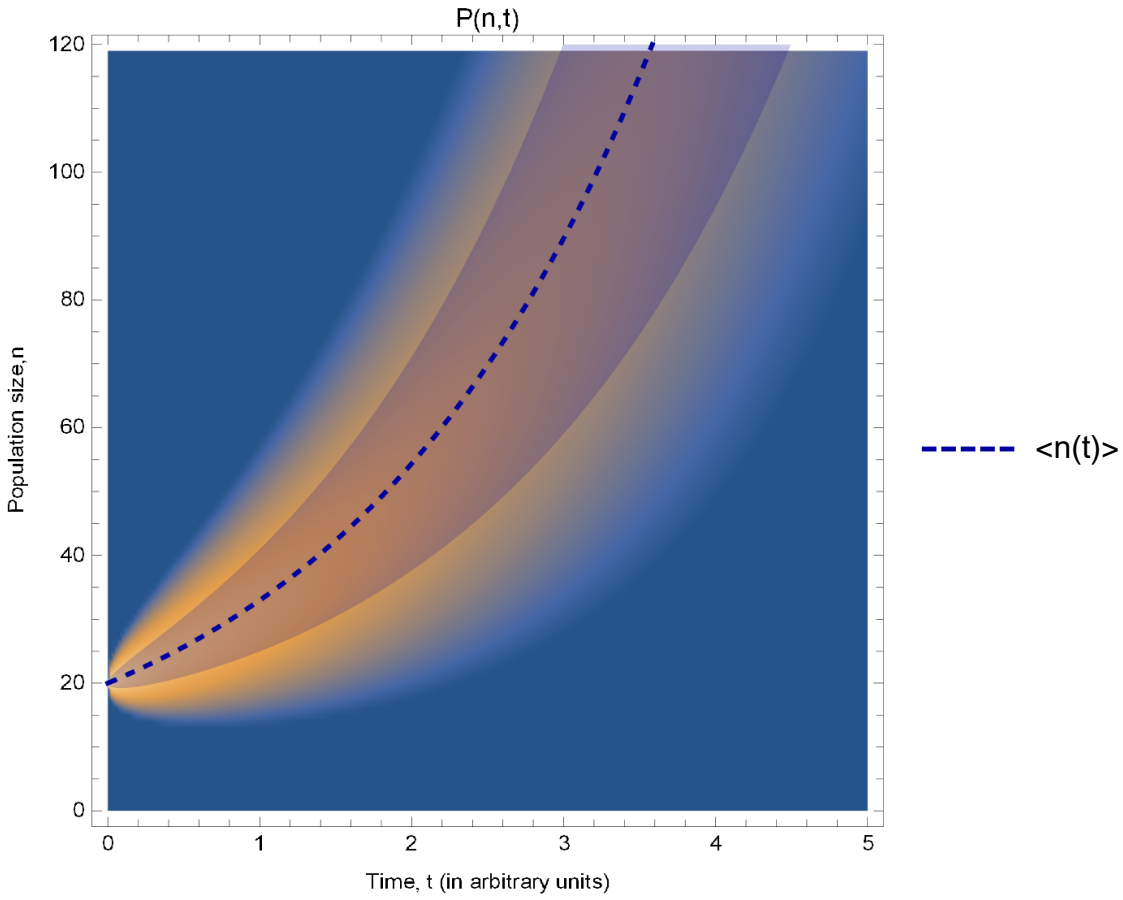

Figure 18: Density plot of $P(n,t)$ together with the computed first moment $< n(t) >$. Deviations of the mean: $< n(t) > \pm$ *standard deviation* are also represented here in this plot by a shadow surrounding the mean.The parameters of the population dynamics are $n_0 = 20$ and $r_{\text{eff}} = \frac{1}{2}$.

3.3.2 Mean Field Theory

You can see that the first two moments provide a lot of information about the underlying stochastic process, which is often enough to answer most of the questions researchers ask about stochastic population dynamics. Moreover, as illustrated by the calculations shown in Section 3.3.1, finding a full solution is, even for the simplest dynamics like the exponential growth discussed here, a tedious and often impossible mission.

As an alternative to finding the full solution of the Master equation, many approximations have been developed [22][23][25]. The simplest one is the mean-field theory approximation which is based on calculating a moment considering each greater moment equal to zero. This approach gets better as the number n of members in our community tends to infinity.

Let us take for example the exponential growth and compute its mean. We have the master equation:

$$\frac{dP(n,t)}{dt} = -\ P(n,t)n(b+d) + P(n+1,t)(n+1)\ d + P(n-1,t)\ (n-1)\ b. \tag{3.28}$$

From it, we get an evolution equation for the mean $< n(t) >$:

$$\begin{aligned}
\frac{d}{dt} < n(t) > &= \sum_n n\frac{dP(n,t)}{dt} \\
&= \sum_n (-n\ P(n,t)n(b+d) + n\ P(n+1,t)(n+1)\ d + n\ P(n-1,t)\ (n-1)\ b) \\
&= \sum_n (-n\ P(n,t)n(b+d) + (n-1)P(n,t)n\ d + (n+1)\ P(n,t)\ n\ b) \\
&= \sum_n P(n,t)n(b-d) \\
&= < n(t) >\ \ (b-d),
\end{aligned} \tag{3.29}$$

which is the same differential equation we introduced in Section 3.4 and whose solution is:

$$< n(t) >= n_0 e^{(b-d)t}. \tag{3.30}$$

The exponential growth is an excellent example to illustrate the agreement between the mean field approximation and the full solution obtained from the Master equation in terms of the generating function.

The mean-field theory approximation is particularly useful for nonlinear master equations, where the generating function method is difficult to handle analytically. Remember the master equation for microscopic dynamics with competition:

$$\begin{aligned}\frac{dP(n,t)}{dt} =& - P(n,t)\left(n\ b + n\ d + \binom{n}{2}\ c\right) \\ &+ P(n+1,t)\left((n+1)\ d + \binom{n+1}{2}\ c\right) + P(n-1,t)\ (n-1)\ b.\end{aligned} \tag{3.31}$$

From it we get a nonlinear differential equation for $< n(t) >$:

$$\begin{aligned}\frac{d}{dt} < n(t) > =& \sum_n n\frac{dP(n,t)}{dt} \\ =& - \sum_n nP(n,t)\left(n\ b + n\ d + \binom{n}{2}\ c\right) \\ &+ \sum_n nP(n+1,t)\left((n+1)\ d + \binom{n+1}{2}\ c\right) \\ &+ \sum_n nP(n-1,t)\ (n-1)\ b \\ =& - \sum_n nP(n,t)\left(n\ b + n\ d + \binom{n}{2}\ c\right) \\ &+ \sum_n (n-1)P(n,t)\left(n\ d + \binom{n}{2}\ c\right) \\ &+ \sum_n (n+1)P(n,t)\ n\ b \\ =& \sum_n P(n,t)\left(n\left(b - d + \frac{c}{2}\right) - n^2\frac{c}{2}\right) \\ =& < n(t) > \left(b - d + \frac{c}{2}\right) - < n^2(t) > \frac{c}{2}.\end{aligned} \tag{3.32}$$

However, notice that this differential equation for the first moment is coupled to the second moment. If we now derive an ODE for the evolution of the second moment, we would find

that it is coupled with the higher moments. In general, we will obtain an infinite system of coupled ODEs. In order to break that coupling and make the equations solvable, we want to neglect the role of fluctuations. For instance, to obtain the evolution of the first moment we set the second moment about the mean (also know as variance) to zero such that $< n^2(t) > \approx < n(t) >^2$:

$$\frac{d}{dt} < n(t) > = < n(t) > \left(b - d + \frac{c}{2}\right) - < n(t) >^2 \frac{c}{2} \tag{3.33}$$

Now, we have a differential equation that can be analytically analyzed, having as solution:

$$< n(t) > = \frac{\left(b - d + \frac{c}{2}\right) n_0 e^{\left(b-d+\frac{c}{2}\right)t}}{\frac{c}{2} n_0 \left(e^{\left(b-d+\frac{c}{2}\right)t} - 1\right) + \left(b - d + \frac{c}{2}\right)}, \tag{3.34}$$

which results in a logistic growth. We can identify the parameters r and K from a direct comparison between Eq. 3.33 and the standard form of the logistic growth equation [26].

$$\frac{dn(t)}{dt} = r_{\text{eff}}\, n(t) \left(1 - \frac{1}{K} n(t)\right) \tag{3.35}$$

and recover the values of r_{eff} and K from the parameters of our microscopic dynamics:

$$r_{\text{eff}} = b - d + \frac{c}{2} \qquad\qquad K = \frac{2}{c}\left(b - d + \frac{c}{2}\right). \tag{3.36}$$

3.4 Numerical Methods

As we have observed, calculating the probabilities $P(n, t)$ could represent a severe challenge for population dynamics more complex than exponential growth. Even if we can compute the mean and standard deviation of this growth, it would be very welcome to have an alternative method to verify that the distribution of $P(n, t)$ behaves as expected, and this is where a numerical approach to the dynamic is useful. A rigorous and more detailed description of the numerical methods used to simulate stochastic processes can be found in [24]. Here we introduce some of the most interesting for this project.

3.4.1 Brute Force Method

This method, as the section heading suggests, is not efficient but easy to implement, and thus it provides an excellent starting point for discussing the use of numerical methods in stochastic problems. In this approach, we perform several runs which only have in common the initial conditions for the population size $n(0) = n_0$. For each run, we start from n_0 and compute all probabilities to stay or exit this state during a small time interval dt. We call these probabilities transition probabilities. Finally, we generate uniform random number between 0 and 1 and choose one of the transitions based on its weight (i.e. the probability of it occurring compared to all other transition probabilities). We compute several runs and calculate the statistical quantities of interest.

To better understand this method, let us illustrate each of its steps with a particular example. Let us take the microscopic dynamics from Fig(16) and the initial condition n_0. As mentioned above, since we have a specific state, we simply calculate the probability of staying or leaving it. For a state defined by a population size n at time t, we can obtain the population size at $t + dt$ by computing the probabilities of all possible events:

$$\begin{aligned} P_{Birth} &= n\ b\ dt \\ P_{Death} &= n\ d\ dt \\ P_{Competition} &= \binom{n}{2}\ c\ dt \\ P_{Nothing} &= 1 - P_{Birth} - P_{Death} - P_{Competition}. \end{aligned} \tag{3.37}$$

It is worth noting that the smaller the dt we use, the more precise our numerical method will be. However, the smaller dt the less efficient the method will be too, because $P_{nothing}$ in Eq. 3.37 will be larger and there will be more time steps in which the population size remains unaltered. Also, dt must be at least so small that the probability for each event respects $0 < P < 1$.

After computing the transition probabilities in Eq. 3.37, to decide which event to fire and

therefore in which direction the population size is updated, we randomly pick a number u from a uniform distribution between 0 and 1. Next, we check if u follows any of the following conditions, which will also change the value of n accordingly:

$$\begin{aligned} &0 < u < n\ b\ dt : n \to n+1 \\ &n\ b\ dt < u < n\ (b + d + \binom{n}{2}\ c)\ dt : n \to n-1 \\ &n\ (b + d + \binom{n}{2}\ c)\ dt < u < 1 : n \to n. \end{aligned} \tag{3.38}$$

In this way we can compute, from n_0 and step by step, a full realization of the stochastic process as shown in the orange curve in Fig(19) (also called trajectory [24]). The final step is to generate many stochastic trajectories (realizations) and compute the averages of the quantities of interest, as shown in Fig(19). We appreciate that for an average of several runs we obtain a smooth curve that matches the analytic predictions very well.

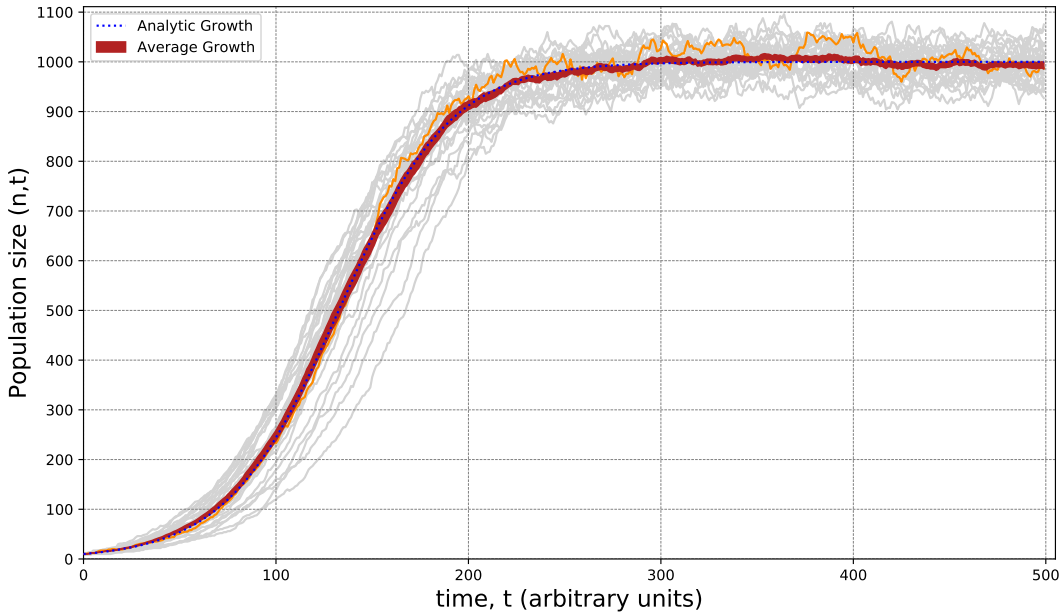

Figure 19: Different realizations of microscopic birth-death-competition dynamics Fig(16) are plot in gray. We compared them with their mean, and with the analytical solution of the mean field equation Eq. 3.34.

3.4.2 Gillespie Algorithm

A method to optimize the algorithm explained above was introduced by Gillespie [27][28]. It is worth noting that it only works for constant rates, which are the cases that we have observed so far.

To observe the difference between the methods, we recall that in the *brute force* method we use a constant time step dt and then evaluate whether or not there is a change in population size at each time step as summarized in Fig(20):

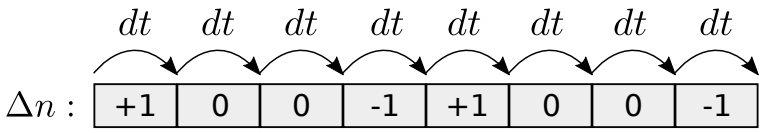

Figure 20: The brute force algorithm evaluates a possible change of state for every dt.

As we already pointed out in Section 3.4.1, as we reduce the size of dt for greater precision, the probability of having an update in population size within each time step also decreases, and thus we compute no transitions most of the time. To avoid these inefficient calculations, the Gillespie method uses and "adaptive" time step dt_{change} which is the time until the next update in population size.

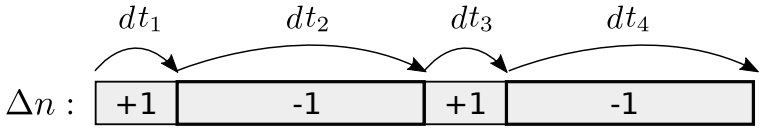

Figure 21: Schematic representation of population updates using the Gillespie algorithm. By using a varying dt, the algorithm avoids evaluating several time steps in which nothing happens to the population.

Therefore, understanding how to calculate the length of the successive time intervals is key to implement this method. More specifically, dt will be a random variable, so we need to calculate the probability distribution for dt. We know that for a population size n the

probability of observing an update in population size per unit of time is given by:

$$r_{total} = n\left(b + d + \binom{n}{2}c\right) \tag{3.39}$$

which is a constant rate until the next event takes place and the population size changes by ± 1. A more rigorous derivation of the distribution followed by the time intervals dt is provided in [24]. To illustrate the principles on which this calculation relies, we will illustrate it using the dynamics with our constant rate r_{total}. Remember that even if n depends on time, in the interval dt of our computations, n can be treated as a constant, since we are computing dt until there is a change in the population size. For a constant rate, we have that the probability of not firing an event by time dt is given by an exponential:

$$P(no\ change_{0\to dt}) = e^{-r_{total}\ dt} \tag{3.40}$$

Now we use Bayes' theorem to compute the probability of the first change event occurring in the time interval $[dt, dt + \delta dt]$[2]:

$$\begin{aligned} P(change_{dt\to dt+\delta dt}) &= \frac{P(change_{dt\to dt+\delta dt}|no\ change_{0\to dt})P(no\ change_{0\to dt})}{P(no\ change_{0\to dt}|change_{dt\to dt+\delta dt})} \\ &= r_{total}\ \delta dt\ e^{-r_{total}\ dt} \end{aligned} \tag{3.41}$$

This is the probability distribution for the time dt when the first change event occurs. However, if we want to use this distribution numerically, we have to map it, ideally, to a uniform distribution from 0 to 1. In our case, we map it to a variable τ with these features:

$$\begin{aligned} d\tau &= -P(change_{dt\to t+\delta dt}) \\ &= -r_{total}\ e^{-r_{total}\ dt}\delta dt. \end{aligned} \tag{3.42}$$

[2]Here we use δdt as a differential of dt in order to avoid writing $d(dt)$ which can be confusing. Recall that dt represents the time interval between two different changing events and comes from a probability distribution.

We can find the map by integration:

$$\tau = e^{-r_{total}\ dt}. \tag{3.43}$$

Finally, as we want to get dt from a uniform distributed τ, we take the inverse of the expression:

$$dt = \frac{1}{r_{total}} ln\left(\frac{1}{\tau}\right) \tag{3.44}$$

Using this expression, we can take a random value for τ and obtain our exponentially distributed value for dt. Now we can evaluate the processes every adaptive dt instead of a fixed one, and we choose which process takes place using another uniformly distributed random variable u from 0 to 1 in the following way:

$$\begin{aligned} &0 < u < \frac{n\ b}{r_{total}} : n \to n+1 \\ &\frac{n\ b}{r_{total}} < u < \frac{n\ (b+d)}{r_{total}} : n \to n-1 \\ &\frac{n\ (b+d)}{r_{total}} < u < 1 : n \to n-1 \end{aligned} \tag{3.45}$$

4 A Model for Aging Population

4.1 Modeling framework

So far we have explored populations with only three processes occurring at the level of the individuals: birth, death, and competition. Accounting for only these three processes, we managed to recover macroscopic dynamics such as exponential and logistic growth that can recapitulate experimental measurements of population growth in some regimes. However, these microscopic dynamics do not take into account the effects of aging and are therefore not useful for tackling our research question and seeking survival benefits in aging populations. Here, we explore two different ways to add the effects of aging to a birth-death-competition dynamics like the one described in previous sections.

We consider a population in which all individuals belong to the same species. In the presence of aging, besides total population size, we need an additional individual-specific degree of freedom to fully describe the population, which is the age of each individual. To make the calculations feasible, we divide our aging population into m different groups, which we call generations,: n_0, n_{-1}, ..., n_{-m}, where the index indicates the amount time that is left until individuals of these generation are born. Therefore, the initial condition is $n_0 = N_0$ and $n_{-i} = 0$ for $i > 0$, which represents an initial population with N_0 members of age zero. We get the age of a sub-population in a group by adding the index i that labels the group they belong to, and time, and thus, for example, the age of n_{-i} at time t is given by $-i + t$. The model equations and initial conditions forbid the presence of individuals with negative age.

In the next three section we explain in detail how the three different microscopic processes (birth, death, and competition) change when we introduce individual ages.

4.1.1 Competition

Furthermore, we have to consider that in the microscopic competition we have different ways in which the members of a sub-population i compete with all the other individuals in the population. They can compete with other members of the i-th group itself in $\binom{n_i}{2}$ ways, and with individuals belonging to any of the different populations j by the product of their populations. In Fig(22) we can observe a summary of all the possible pairs of competing individuals.

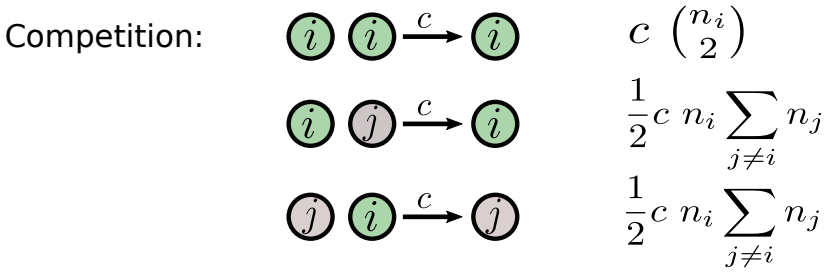

Figure 22: Individuals from the sub-population i compete against other members of the same sub-population i, or against members of any of the other sub-populations j. The right column shows the number of possible pairs of competing individuals for each kind of interaction.

4.1.2 Death Rate and Survivorship

According to the definition of aging we gave in Section 2.1.2, more aged individuals are more likely to suffer from internal malfunctions and die. Therefore, we add an extra, positive contribution to the death rate, d. We do it through a quadratic dependence on age weighted by a parameter λ:

$$d(age) = d_0(1 + \lambda age^2). \tag{4.1}$$

Here we use the quadratic term of age for analytical tractability and because it qualitatively recovers experimental survival curves [17]. However, the dependence between age and death rate is species-specific and thus it should be properly tuned depending on the species that is being studied. The parameter λ controls how much aging, through internal damage, affects

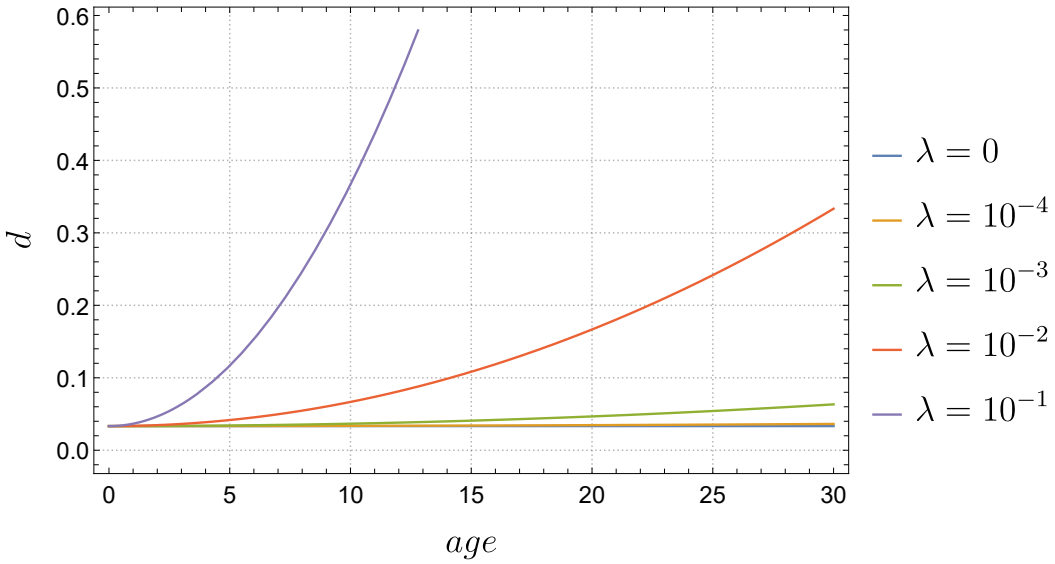

Figure 23: Death rate $d(age)$ vs age for different values of λ. We used $b = 0.23$, $d = 0.033$ and $c = 3.95 \times 10^{-8}$.

the chances of death. For $\lambda = 0$, we have a constant rate and the macroscopic dynamics behave logistically. This scenario reflects the case in which external hazards strongly dominate the death term. In the opposite limit, for $\lambda \gg age^{-2}$, we have populations in which the probability of death is given almost entirely by internal malfunctions. Biologically, these means that individuals in this populations accumulate a lot of internal malfunctions very early in their life, or they have good protection against environmental hazards. One way to compare it with actual biological observations [17] is through the concept of survivorship, a quantity that for living beings with monotonically increasing age can be defined as:

$$s(age) = Max\left(0, 1 - \int_0^{age} d_0(1 + \lambda\ age^2)dx\right), \tag{4.2}$$

where $s(age)$ is the probability of finding the individual alive at a certain age. This is the reason why survivorship is only defined for monotonically increasing age. For $\lambda = 0$ this curve is a straight line with slope λ, and for greater values, it has a faster decay.

Given this modified death rate, we add the effects of aging to the microscopic dynamics shown in Fig(25), where we observe that the total death rate for the sub-population i is given only by age $i + t$ and its total number n_i.

Figure 24: Survivorship (in percentage) vs age. We used $b = 0.23$, $d = 0.033$ and $c = 3.95 \times 10^{-8}$.

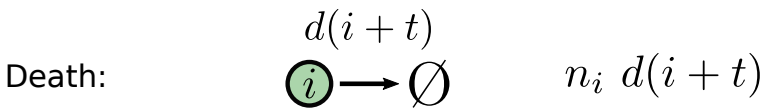

Figure 25: Age effects in the death rate for members of the sub-population i.

4.1.3 Reproduction

Once we consider aging, represented by internal aging, an important question arises related to how this damage is divided among daughter cells upon division. For this we introduce a parameter μ that indicates the fraction of damaged shared with the first child, the damage of the second being $1 - \mu$, as we observe in Fig(26). It is worth noting that from this definition, there is symmetry in μ, so we only need to consider values of μ between 0.5 and 1. $\mu = 0.5$ indicates that the damage is distributed equally among daughters cells, and therefore this is what we call symmetric reproduction. On the other hand, for $\mu = 1$ all the damage goes to one of the daughters, while the other is born without damage. This is the completely asymmetric reproduction, and just in this situation, we can call the original cell, the mother cell.

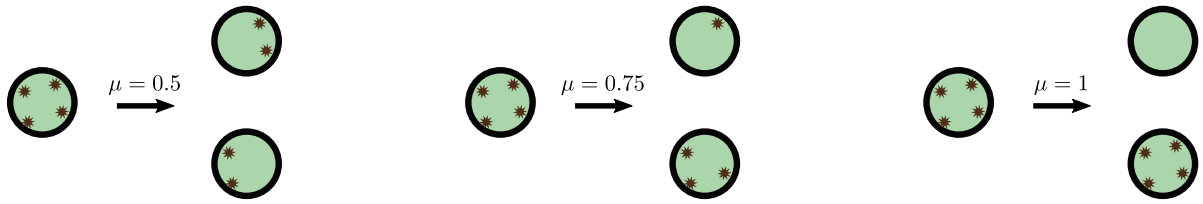

Figure 26: The parameter μ determines how damage is distributed among the daughter cells.

Now we proceed to implement μ in the model. We want a birth process after which a member of one of the sub-populations gives raise to two new individuals that, in principle, will belong to sub-populations that are different to the one the original cell belonged to as shown in Fig(27).

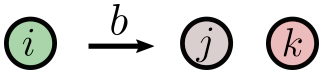

Figure 27: After cell division, one cell from sub-population i gives raise to two cells that. will belong to different sub-populations

At time t, the age of the two new cells must be weighted by a factor μ (or $1-\mu$) to account for the asymmetric division of damage. We write this restriction in the groups new cells can belong to, using Kronecker Delta functions $\delta_{j+t,\mu(i+t)}$ and $\delta_{j+t,\mu(i+t)}$. In this way, for a given asymmetry parameter μ new cells can only belong to the j groups such that the total damage age (or cell damage) is conserved before and after division. Finally, now that we know how a birth process is represented, we look at the different ways in which this dynamic affects a sub-population i. The first and second are ways in which a population i can be the daughter of another population j, and the third is given by the moment when i reproduces.

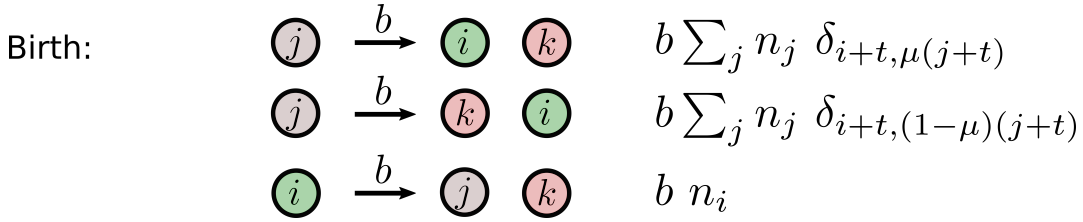

Figure 28: Microscopic reproduction dynamics which affect the i_{th} sub-population.

4.1.4 Master Equation

Putting together every possible transitions detailed above and summarized in Fig(29), we can write a master equation for the probability of having n_i individuals in group i at time t.

$$\frac{d}{dt}P(n_i,t) = \underbrace{bP(n_i+1,t)(n_i+1)}_{\text{Probability of having } n_i+1 \text{ followed by a reproductive event in sub-population } i.}$$

$$\underbrace{+bP(n_i-1,t)\sum_j \left(\delta_{i+t,\mu(j+t)} + \delta_{i+t,(1-\mu)(j+t)}\right) < n_j(t) >}_{\text{Reproductive event in sub-population } j \text{ that adds one daughter cell in the } n_i-1 \text{ sub-population } i.}$$

$$\underbrace{-bP(n_i,t)n_i}_{\text{Reproductive event in } i \text{ that subtract one individual from the } n_i+1 \text{ members.}}$$

$$\underbrace{-bP(n_i,t)\left(\sum_j \left(\delta_{i+t,\mu(j+t)} + \delta_{i+t,(1-\mu)(j+t)}\right) < n_j(t) >\right)}_{\text{A daughter cell from } j \text{ adds one individual to the } n_i \text{ members of the sub-population } i.}$$

$$\underbrace{+dP(n_i+1,t)(i+t)(n_i+1)}_{\text{An } i_{th} \text{ population with } n_i+1 \text{ members loses one individual.}} \tag{4.3}$$

$$\underbrace{-dP(n_i,t)(i+t)n_i}_{\text{An original } n_i \text{ sub-population decreases by 1 for a death process.}}$$

$$\underbrace{+cP(n_i+1,t)\left(\binom{n_i+1}{2} + \frac{1}{2}(n_i+1)\sum_{j\neq i} < n_j(t) >\right)}_{\text{The group } n_i+1 \text{ loses an individual by competition against the same group and the others.}}$$

$$\underbrace{-cP(n_i,t)\left(\binom{n_i}{2} + \frac{1}{2}n_i\sum_{j\neq i} < n_j(t) >\right)}_{\text{One of the } n_i \text{ members of } i \text{ dies due to competition against another member of the population.}}$$

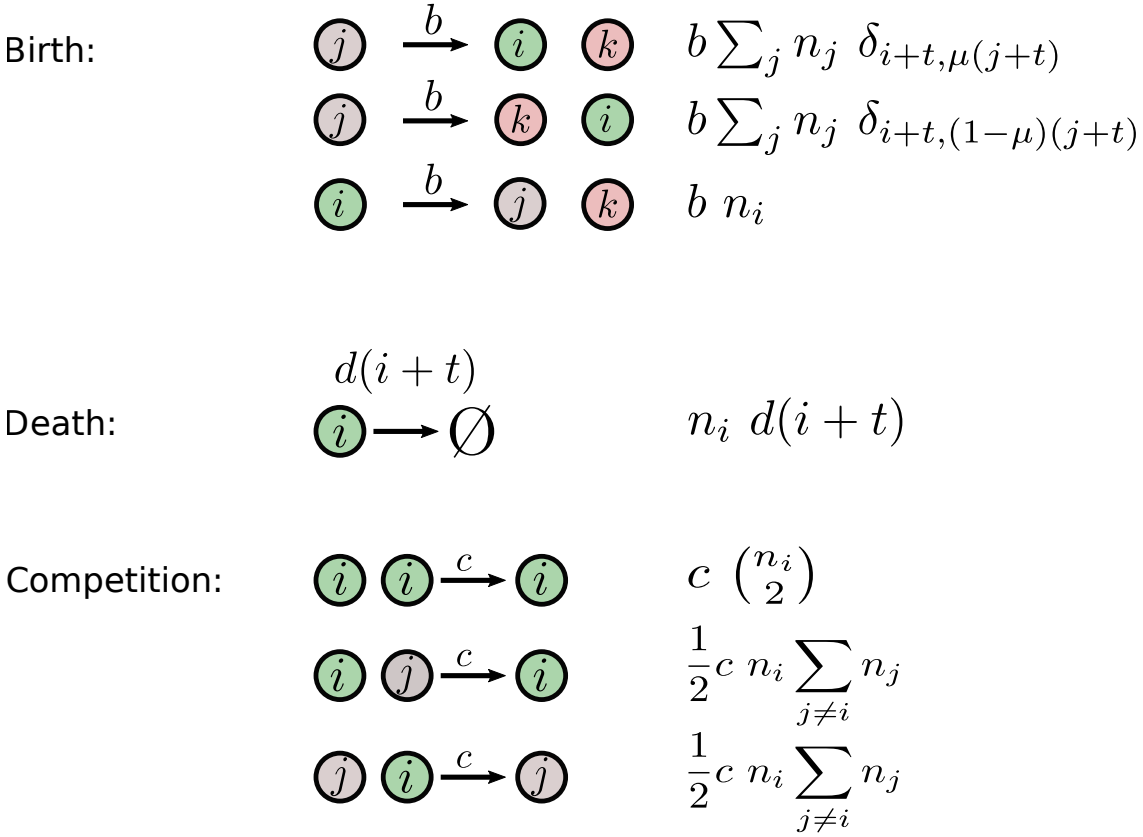

Figure 29: Microscopic dynamics for an aging i_{th} sub-population.

4.2 Methods to analyze the model.

4.2.1 Numerical Methods: the tRSSA Algorithm

As we discussed in section 3.4.2, the Gillespie algorithm only works when events at the microscopic scale (birth/death/competition) occur at constant rate. In the presence of aging, this condition is violated, as it can be clearly seen from the definition of the death rate. Therefore, we must adapt Gillespie's algorithm to work with time-dependent rates. Being familiar with the derivation of Gillespie's algorithm, this generalization is not hard. First, we compute the probability that nothing changes in a time interval $[0, dt]$ [29]:

$$P(no\ change_{0\to dt}) = e^{-\int_{dt'=0}^{dt} r_{total}(dt')\ d(dt')}. \tag{4.4}$$

where $r_{total(dt')}$ is our total rate given by the addition of the term in the right column of Fig(29). The total rate is now time dependent. Applying Bayes' theorem, we can obtain the probability to change in $[dt, dt + d(dt)]$:

$$P(change_{dt \to dt+d(dt)}) = r_{total}(dt) e^{-\int_{dt'=0}^{dt} r_{total}(dt') d(dt')} d(dt) \tag{4.5}$$

In a similar way to Gillespie, we map the probability to a uniform distributed variable τ:

$$d\tau = -P(change_{dt \to dt+d(dt)}). \tag{4.6}$$

Remember that the minus sign comes from the different direction in the real axis when mapping dt from 0 to ∞ into τ from 1 to 0. Plugging Eq. 4.5 into Eq. 4.6 and after integrating the last we recover an expression relating dt with the random, uniformly distributed variable τ:

$$\int_{dt'=0}^{dt} r_{total}(dt') d(dt') = ln\left(\frac{1}{\tau}\right) \tag{4.7}$$

However, we have not isolated dt like we were able in Gillespie. Moreover, Eq. 4.7 contains an integral that can be problematic in certain scenarios. To avoid this problem, we implement the *time-dependent rejection-based stochastic simulation algorithm (tRSSA)* which is a rejection-based generalization of the Gillespie algorithm introduced in [29].

There are two main differences beween tRSSA and the Gillespie method. First of all, tRSSA is a rejection-based stochastic simulation algorithm [30][31][32], where it is not necessary to compute transition probabilities at every dt.

For instance, consider a process whose transition probability is given by $f(n)\ b$, with f an increasing function of the number of individuals n. Birth in cells is a specific case of this process, where $f(n) = n$. In Gillespie, we compute the value of $f(n)$ at every time step dt_i: $f(n(t_1))\ b$, $f(n(t_2))\ b$, $f(n(t_3))\ b$, ..., $f(n(t_n))\ b$. However, tRSSA avoids this explicit computation by using a value for n_{min} and n_{max}, so $n_{min} < n < n_{max}$, and therefore

$f(n_{min}) < f(n) < f(n_{max})$.

With n bounded, we perform an i_{th} rejection step by taking a random number τ_i and add it to dt, which is initially zero:

```
dt = dt + math.log(1/tau[i])/(f(nmax)*b).
```

After updating the time step dt, it is time to check if a transition event will fire or not. To do so we randomly pick a number r and check if $r < \frac{f(n_{min})}{f(n_{max})}$. We fire this event if we meet the condition, and just when this condition is not true, we compute the exact value of $f(n)\ b$ and check if $r < \frac{f(n)\ b}{f(n_{max})\ b}$ to see if it actually fires or not. This is why we call every step a rejection step, and for appropriate values of n_{min} and n_{max} the chances we actually compute $f(n)\ b$ diminishes considerably.

We continue performing rejection steps until a transition event is triggered. Once the event fires, we change n according to this event and increase the time by dt. Finally we verify if n is still in the boundary, updating the bounds in case it is not, and reinitializing $dt = 0$ for the next loop as well as the index i. We observe that for appropriate bounds, we do not need to compute $f(n)\ b$ explicitly, and only the values of the limits $f(n_{min})\ b$ and $f(n_{max})\ b$ are sufficient, making the simulation more efficient for more complicated functions f.

To add time dependency, tRSSA discretizes time in a list t_ℓ and verifies that $t_\ell < t + dt < t_{\ell+1}$ in every rejection step i. If this condition is false, we update the probabilities, specifically the rates which are time dependent, before starting the next rejection step. Let us take for instance the previous example but with a time dependent rate $b(t)$. In every rejection step we now bound not only the population number $n_{min} < n < n_{max}$, but the total propensity. For instance, for an increasing function $b(t)$, these bounds can are $f(n_{min})\ b(t_\ell) < f(n)\ b(t) < f(n_{max})b(t_{\ell+1})$.

4.2.2 Analytic Approach

Even wit tRSSA, to simulate larger population size, as expected for microbial systems,is computationally challenging. For this reason we developed an analytical approach to obtain the mean values of the stochastic process and use the numerical method to verify them. From the master equation Eq. 4.3, we compute using the mean field theory approach the dynamics for $< n_i(t) >$:

$$\begin{aligned}\frac{d < n_i(t) >}{dt} = b\left(\sum_j \left(\delta_{i+t,\mu(j+t)} + \delta_{i+t,(1-\mu)(j+t)}\right) < n_j(t) > - < n_i(t) >\right) \\ - < n_i(t) > d(i+t) + \frac{c}{2} < n_i(t) > - \frac{c}{2} < n_i(t) > \sum_j < n_j(t) >\end{aligned} \tag{4.8}$$

Let us define the total population as $N(t) = \sum_i n_i(t)$. We are able to get an expression for the stationary value of $N(t)$: N_F, by adding over all possible sub-populations and then making its temporal derivative equal to zero:

$$< N_F > = < N_{Fd_0} > -2\frac{d_0\lambda}{c} < age^2 > . \tag{4.9}$$

Here N_{d_0} is the stationary population for $\lambda = 0$. This is a very interesting result, telling us how the total population size in the stationary state (system carrying capacity) is affected by aging. In a more general scenario, for a death rate given by:

$$d(age) = d_0(1 + \lambda f(age)) \tag{4.10}$$

the population size will be:

$$< N_F > = < N_{Fd_0} > -\frac{2\ d_0\ \lambda}{c} < f(age) > . \tag{4.11}$$

We can also compute the population in the stationary-state through its distribution on age. In this state, we expect that the population size for each age to be constant regardless

of the time at which it is measured. Therefore:

$$< n_i(t) >=< n_{i-dt}(t+dt) > . \tag{4.12}$$

It allows us to get an expression for the time derivative of $< n_i(t) >$:

$$\begin{aligned} \frac{d}{dt} < n_{i-dt}(t) > &= \frac{< n_{i-dt}(t+dt) > - < n_{i-dt}(t) >}{dt} \\ &= \frac{< n_i(t) > - < n_{i-dt}(t) >}{dt}, \end{aligned} \tag{4.13}$$

which will be useful after replacing it in Eq. 4.8:

$$\begin{aligned} < n_i(t) > &= < n_{i-dt}(t) > \\ &+ bdt \left(\sum_j \left(\delta_{i-dt+t,\mu(j+t)+} + \delta_{i-dt+t,(1-\mu)(j+t)} \right) < n_j(t) > - < n_{i-dt}(t) > \right) \\ &- < n_{i-dt}(t) > d(i-dt+t)dt + \frac{c}{2} dt < n_{i-dt}(t) > \\ &- \frac{c}{2} dt < n_{i-dt}(t) > \sum_j < n_j(t) > . \end{aligned} \tag{4.14}$$

These equations can be solved algebraically to obtain the distribution of ages within the population for different values of μ. For example we show the distributions for the extreme cases of μ in Fig(30). It is worth noting that, from the age distribution, we can get the total population size in the stationary state as a function of the model parameters $N_F(\lambda, \mu)$, after adding all $n_i(t_{stationary})$. In this way we can verify the relation between N_F and $< age^2 >$ derived in Eq. 4.9 as well as the numerical simulations using the tRSSA algorithm (Fig(32) and Fig(31)).

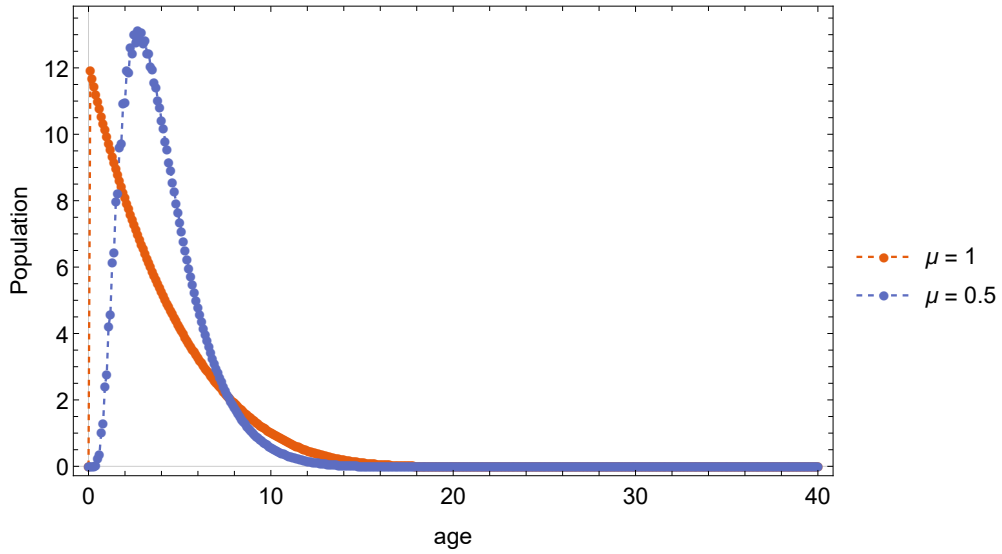

Figure 30: Distribution of ages within the population for symmetric ($\mu = 0.5$) and asymmetric ($\mu = 1$) reproduction. Here we used $b = 0.23$, $c = 0.000129$, and $d_0 = 0.1667$. The value of λ is 0.008 and each age bin has a width of 0.1.

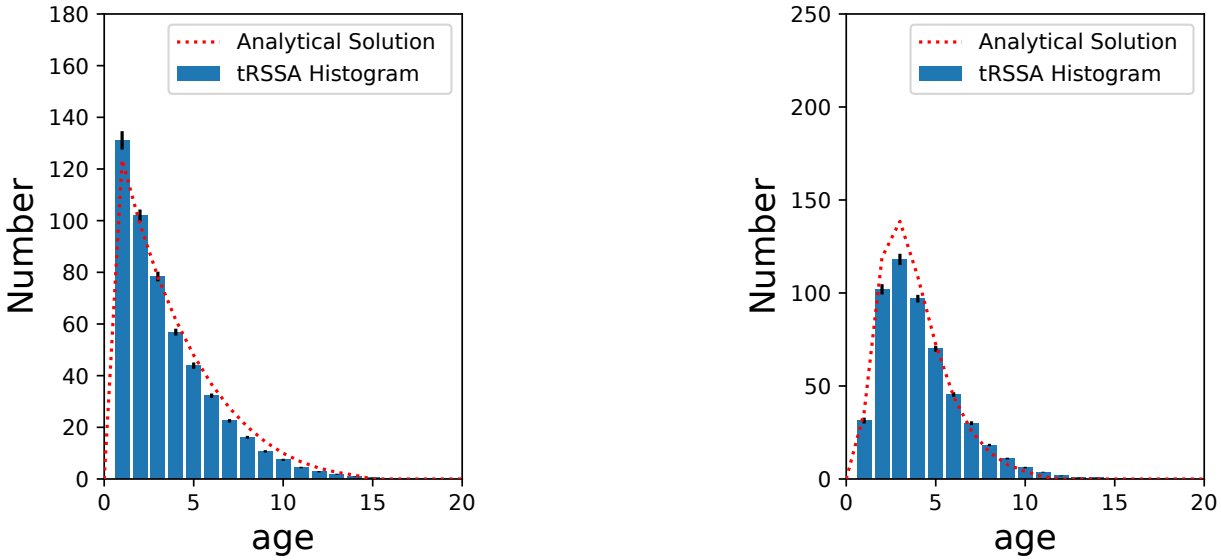

Figure 31: Distribution of ages within the population for completely asymmetric reproduction $\mu = 1$ on the left and symmetric reproduction $\mu = 0.5$ on the right. We compare our numerical solution using tRSSA with our analytic results.Here we used $b = 0.23$, $c = 0.000129$, and $d_0 = 0.1667$. The value of λ is 0.008 and each age bin has a width of 1, this is why the values are 10 times large than in Fig(30).

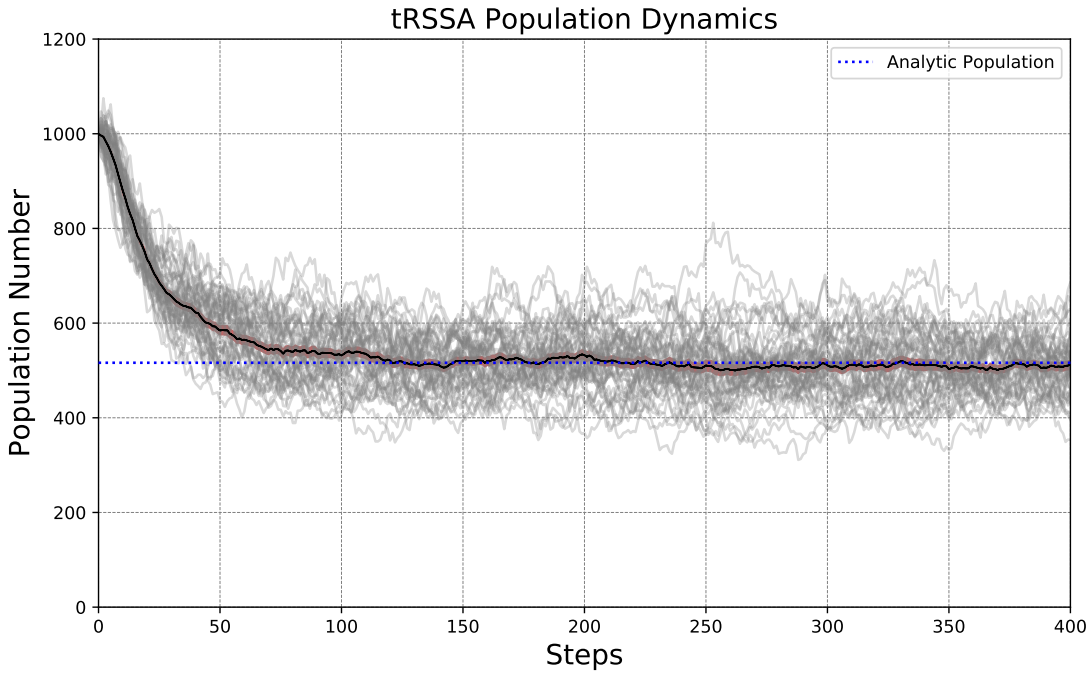

Figure 32: Total population vs time as simulated using tRSSA. Each gray line represents an independent realization, the black line is the mean and the red around represents one standard deviation. We compare the final value with our analytic result. Here we used $b = 0.23$, $c = 0.000129$, and $d_0 = 0.1667$. The value of λ is 0.008 and $\mu = 1$.

5 Results: To be Mortal or Immortal

5.1 Comparison Between Strategies

With the help of numerical methods to verify the precision of our analytic expressions, we proceed to explore the effects of different values of μ and λ in the population dynamics, and, more specifically, on the total population size and the age composition in the stationary state.

We explore the effect of asymmetry in the distribution of damage on the variability of age in the population. We expect to find that that a larger μ represents a greater variation in age, which is what we call aging, while a μ closer to 0.5 has a more restricted age range, being this what we have defined as immortality in Section 2. As we observe in Fig(33) for many different values of λ, the standard deviation of age σ monotonically increases with μ confirming our statement.

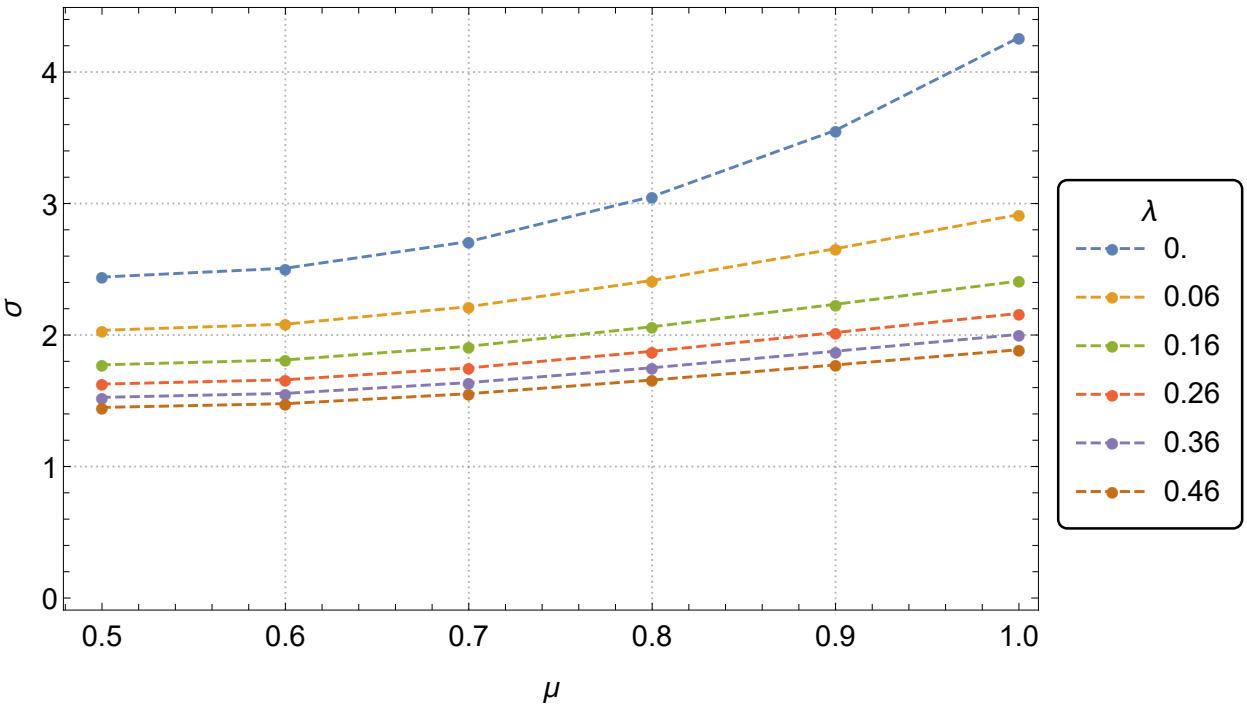

Figure 33: For fixed λ we observe and increasing standard deviation σ as μ increases. We used $b = 0.23$, $c = 3.95 \times 10^{-8}$, and $d_0 = 0.0333$.

Next, we study the steady-state total population size for different sets of parameters (μ, λ). We start with simulations for different values of λ, establishing that for $\lambda = 0$ the carrying capacity N_F must be equal to 10^7. We note in the Fig(34) that for a long value of λ, a completely asymmetric reproduction is very advantageous, and even survives extinction for values of λ in which the symmetric spawning population does not. Nevertheless, for small values of λ this behavior is reversed, and a symmetric distribution of damage leads to larger population sizes. However, it is not that noticeable as for low values of λ total population sizes are large for every μ. This switch in the value of μ that leads to larger population sizes is more easily appreciated when we explore $\sqrt{< age >^2}$ and the relationship:

$$< N_F >=< N_{F d_0} > -2\frac{d_0 \lambda}{c} < age^2 > . \tag{5.1}$$

From Eq. 5.1, we can see that the smaller values of $< age^2 >$, given a constant λ, represent larger final populations. As we see in Fig(35), for small λ, the totally asymmetric reproduction λ has the largest $< age^2 >$, which will make the totally asymmetric strategy to achieve smaller population sizes than those reached by the symmetric strategy. On the other hand, we have the opposite relation for larger values of λ. In this scenario, completely asymmetric reproduction leads to larger steady-state population sizes than a fully symmetric distribution of damage.

Finally, to show how mortality affects total population sizes in the stationary state, we reproduce in Fig(36) the steady-state total population size N_F against the degree of asymmetry in reproduction μ. As mentioned above, from here we see that the effect of an asymmetric distribution of damage on the total population size is stronger for larger λ, and that in this scenario having a larger μ can prevent the population from extinction.

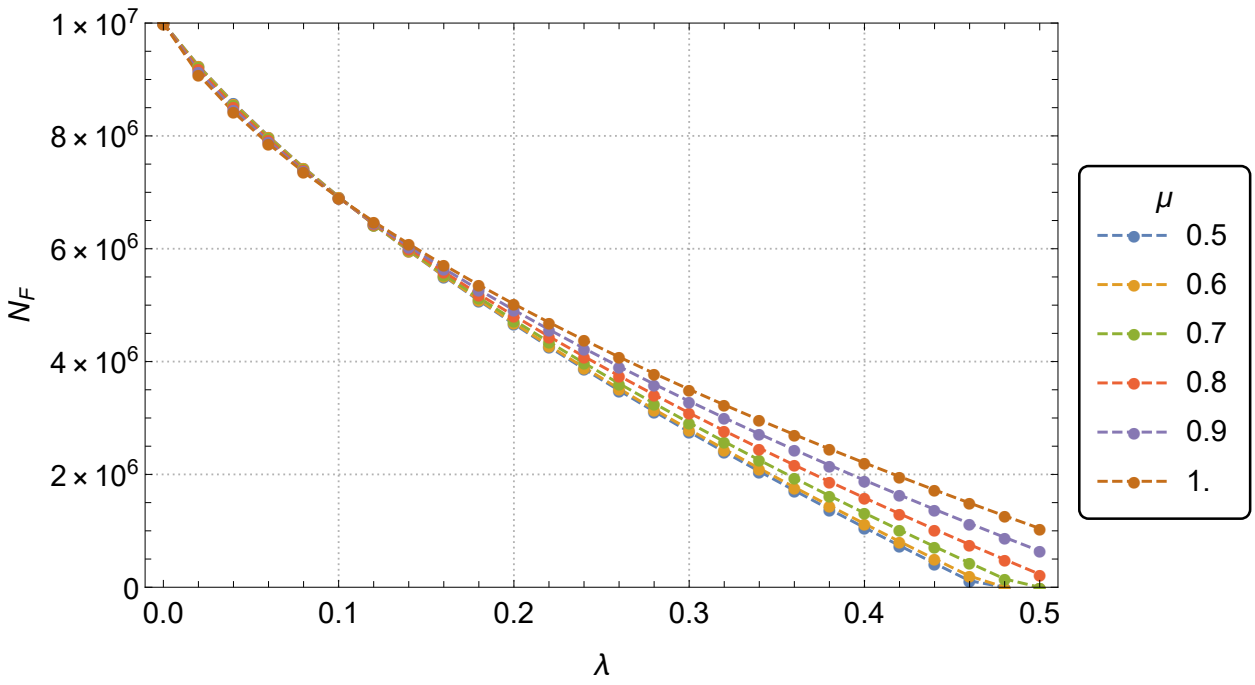

Figure 34: Stationary population for different values of λ. We observe that, for value where the population is in risk, i.e. larger values of λ, a asymmetric strategy is more advantageous. We used $b = 0.23$, $c = 3.95 \times 10^{-8}$, and $d_0 = 0.0333$.

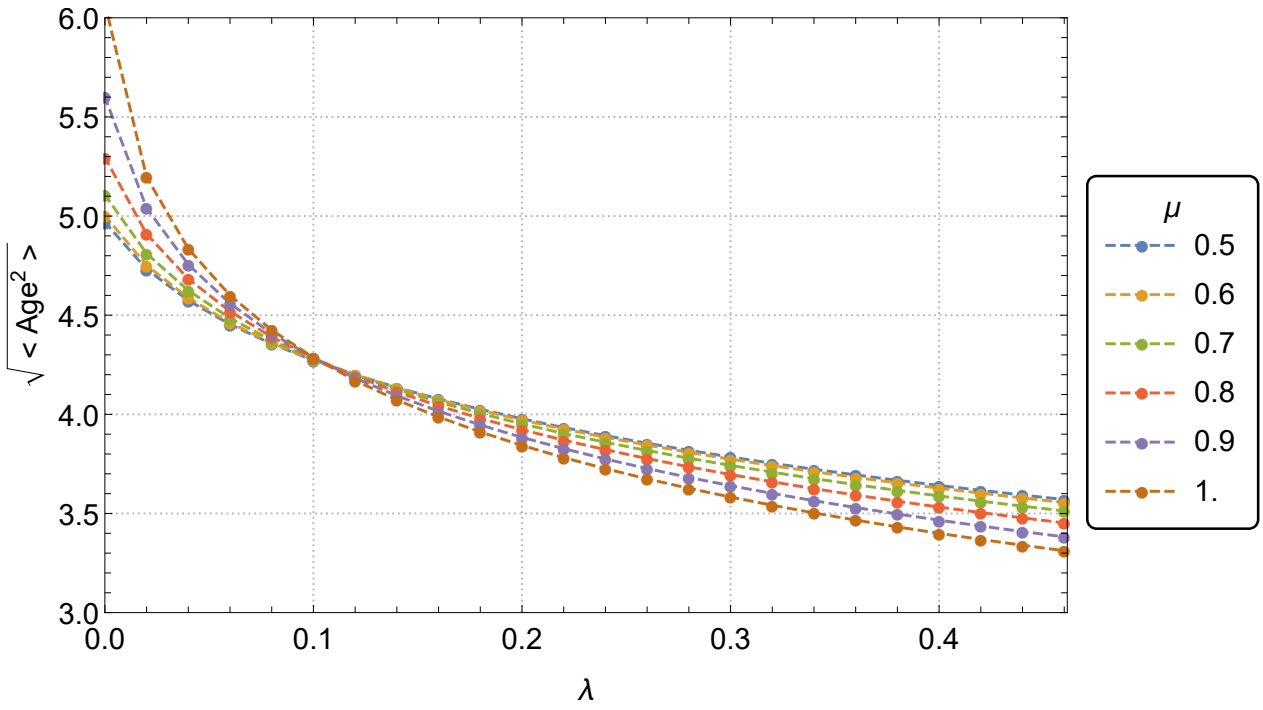

Figure 35: $\sqrt{< age^2 >}$ of populations vs λ. Here we are able to appreciate in a better way the transition from symmetric being the most advantageous reproduction to the least advantageous one as λ increases. We used $b = 0.23$, $c = 3.95 \times 10^{-8}$, and $d_0 = 0.0333$.

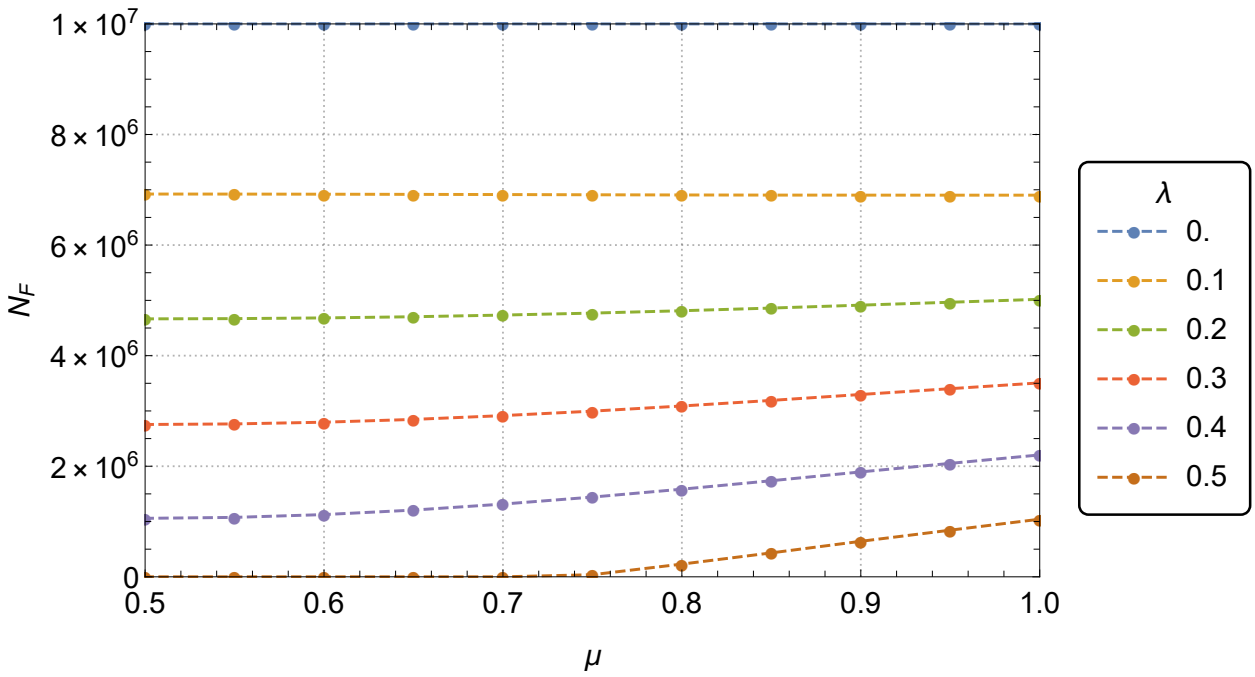

Figure 36: Steady-state total population size vs the reproduction strategy. We observe that for small values of N_F and constant λ, asymmetric reproduction has advantages over the symmetric one. We used $b = 0.23$, $c = 3.95 \times 10^{-8}$, and $d_0 = 0.0333$.

5.2 Summary, discussion and future steps

In this thesis we have presented a new theoretical framework to study the effect of aging on the survival of a microbial population. To construct this model, we departed from the three basic ingredients that are considered in traditional in the traditional logistic model (reproduction, death and competition) and extended that number of processes to account for the effect of aging. This model was analyzed by a combination of numerical simulation and mean-field calculations.

We observed that, for populations in which λ is large, a total asymmetric reproduction is advantageous because, in the long term, it leads to larger population sizes. From it, we can interpret that, for species in which aging does not affect their lifestyle much, being immortal or not, does not have a big impact in the total population, as we expected. However, if aging has a great effect in the population, to have a completely asymmetric distribution of cell damage upon division turns out to be the best reproductive strategy for the population.

This may seem counter-intuitive at first, however, it is related to the fact that populations following a completely asymmetric reproduction have many more younger individuals than symmetrical ones, and for this reason, they have a better chance of surviving and maintaining a larger number.

It is important to highlight, however, that this relation between maximum steady-state total population size and degree of asymmetry in the reproduction does depend on λ. For low values of λ, a symmetric distribution of damaged leads to larger population sizes than an asymmetric one. Importantly, however, the positive effect of an asymmetric distribution of damage on the steady-state population size appears for large values of λ, for which the population is closer to extinction. This result raises important questions about the reasons why more species with these strategies have survived and outnumbered the symmetric strategic ones.

Besides being interesting by themselves, the results presented in this thesis open a larger number of questions deserving further exploration. We observe in Fig(35) a transition in λ at which a fully symmetric distribution of damage shifts from being the most advantageous strategy to the least advantageous. Future research could focus on exploring how this transition changes as a function of λ and μ. Specifically, it would be interesting to investigate whether there are model parametrizations in which this transition is located further to the right in Fig(35), i.e. at larger enough values of λ. To find this would represent cases in which symmetrical reproduction is more advantageous than a fully asymmetrical one to prevent extinction. However, we have not found it so far. This phenomena would be reflected as a change of slope of the N_F curve for large values of λ in Fig(36).

References

[1] Theodosius Dobzhansky. Nothing in biology makes sense except in the light of evolution. *Am Biol Teach*, 35:125–29, 03 1973.

[2] Josh Mitteldorf. *Evolutionary Origins of Aging*, pages 87–126. 12 2009.

[3] Jicun Wang-Michelitsch and Thomas Michelitsch. Misrepair accumulation theory: a theory for understanding aging, cancer development, longevity, and adaptation. 05 2015.

[4] Thiago Monaco and Paulo Silveira. Aging is not senescence: A short computer demonstration and implications for medical practice. *Clinics (São Paulo, Brazil)*, 64:451–7, 11 2009.

[5] Jicun Wang, Thomas Michelitsch, Arne Wunderlin, and Ravi Mahadeva. Aging as a consequence of misrepair – a novel theory of aging. *Nature Precedings*, 04 2009.

[6] Huba Kiss, Agoston Mihalik, Tibor Nánási, Bálint Őry, Zoltan Spiro, Csaba Sőti, and Peter Csermely. Ageing as a price of cooperation and complexity. *BioEssays : news and reviews in molecular, cellular and developmental biology*, 31:651–64, 06 2009.

[7] Thomas Kirkwood. Understanding the odd science of aging. *Cell*, 120:437–47, 03 2005.

[8] Alexey Moskalev. Evolutionary ideas on the nature of aging. *Advances in gerontology = Uspekhi gerontologii / Rossiiskaiaa akademiia nauk, Gerontologicheskoe obshchestvo*, 1:112–121, 04 2011.

[9] Andre Martins. Change and aging senescence as an adaptation. *PloS one*, 6:e24328, 09 2011.

[10] Jicun Michelitsch-Wang and Thomas Michelitsch. Traditional aging theories: which ones are useful? 03 2015.

[11] Annette Baudisch. How ageing is shaped by trade-offs. *Max Planck Institute for Demographic Research, Rostock, Germany, MPIDR Working Papers*, 01 2009.

[12] Alexei Maklakov and Tracey Chapman. Evolution of ageing as a tangle of trade-offs: Energy versus function. *Proceedings of the Royal Society B: Biological Sciences*, 286:20191604, 09 2019.

[13] Thomas Wilhelm, Jonathan Byrne, Rebeca Medina, Ena Kolundzic, Johannes Geisinger, Martina Hajduskova, Baris Tursun, and Holger Richly. Neuronal inhibition of the autophagy nucleation complex extends life span in post-reproductive c. elegans. *Genes & development*, 31, 09 2017.

[14] L Partridge and N Barton. Optimality, mutation and the evolution of aging. *Nature*, 362:305–11, 04 1993.

[15] David Kysela, Pamela Brown, Kerwyn Huang, and Yves Brun. Biological consequences and advantages of asymmetric bacterial growth. *Annual review of microbiology*, 67, 06 2013.

[16] Thomas Kirkwood. Asymmetry and the origins of ageing. *Mechanisms of ageing and development*, 126:533–4, 06 2005.

[17] Roy Moger-Reischer and Jay Lennon. Microbial ageing and longevity. *Nature Reviews Microbiology*, 17:1–12, 09 2019.

[18] Eric Stewart, Richard Madden, Gregory Paul, and Francois Taddei. Aging and death in an organism that reproduces by morphologically symmetric division. *PLoS biology*, 3:e45, 03 2005.

[19] Martin Nowak. *Evolutionary Dynamics: Exploring the Equations of Life*, volume 82. 01 2007.

[20] Marcel Zwietering, I Jongenburger, F.M. Rombouts, and Talya Van. Modeling of bacterial growth curve. *Applied and environmental microbiology*, 56:1875–81, 07 1990.

[21] Jianping Xu. Reproduction and sex in microorganisms. *Encyclopedia of life supporting systems. UN-UNESCO*, 2009.

[22] Crispin W Gardiner et al. *Handbook of stochastic methods*, volume 3. springer Berlin, 1985.

[23] Nicolaas Godfried Van Kampen. *Stochastic processes in physics and chemistry*, volume 1. Elsevier, 1992.

[24] Raúl Toral and Pere Colet. *Stochastic numerical methods: an introduction for students and scientists*. John Wiley & Sons, 2014.

[25] Luis F Lafuerza and Raul Toral. On the gaussian approximation for master equations. *Journal of Statistical Physics*, 140(5):917–933, 2010.

[26] James D Murray. *Mathematical biology: I. An introduction*, volume 17. Springer Science & Business Media, 2007.

[27] Daniel T. Gillespie. A General Method for Numerically Simulating the Stochastic Time Evolution of Coupled Chemical Reactions. *Journal of Computational Physics*, 22(4):403–434, December 1976.

[28] Daniel T. Gillesple and Danlel T. Gillespie. Exact stochastic simulation of coupled chemical reactions.

[29] Vo Thanh and Corrado Priami. Simulation of biochemical reactions with time-dependent rates by the rejection-based algorithm. *The Journal of chemical physics*, 143:054104, 08 2015.

[30] Rajesh Ramaswamy, Nélido González-Segredo, and Ivo Sbalzarini. A new class of highly efficient exact stochastic simulation algorithms for chemical reaction networks. *The Journal of chemical physics*, 130:244104, 07 2009.

[31] Vo Thanh, Corrado Priami, and Roberto Zunino. Efficient rejection-based simulation of biochemical reactions with stochastic noise and delays. *The Journal of chemical physics*, 141:134116, 10 2014.

[32] Vo Thanh, Roberto Zunino, and Corrado Priami. On the rejection-based algorithm for simulation and analysis of large-scale reaction networks. *The Journal of Chemical Physics*, 142:–, 06 2015.